November 2022

Aldosterone Treatment Protects Connexin 30 and 43 Expression for Age-Related Hearing Loss

Jennifer A. Pineros Valencia
University of South Florida

Aldosterone Treatment Protects Connexin 30 and 43 Expression for Age-Related Hearing Loss

by

Jennifer A. Pineros Valencia

A dissertation submitted in partial fulfillment
of the requirements for the degree of
Doctor of Philosophy
Department of Medical Engineering
College of Engineering
University of South Florida

Major Professor: Robert Frisina, Ph.D.
Bo Ding, M.D.
Victoria Sanchez, Ph.D.
Mark Jaroszeski, Ph.D.
Nathan Gallant, Ph.D.

Date of Approval:
November 17, 2022

Keywords: Connexins, Presbycusis, Kir4.1, Aging, Drug Development

Dedication

I dedicate this dissertation to my family and friends. Every single one of you has helped me achieve my dream. For that, thank you. I'll forever be grateful for all of your support.

Mami y Papi, gracias por todo lo que han hecho por mí. Este logro es gracias a ustedes y para ustedes. Words fail me in explaining how much I appreciate every sacrifice you have made for me to achieve this long-awaited goal; this is all thanks to you. Stephanie, being your older sister has not only been a huge blessing, but it's also been the greatest motivation as I hope this shows you that anything is possible. To my brother, I hope your little sister made you proud. And a special shoutout to my dogs. Snoopy and Minnie, thank you for almost 10 years of unconditional love and for being the best study buddies.

A mi Abuelita Blanca, gracias por todas tus bendiciones. ¡Y mira Abuela, ya llegué al último escalón! A mi Abuelita Ana, que yo sé que me ha estado mirando desde el cielo durante todos estos años, espero que te he llenado de orgullo. And to all my aunts, uncles, cousins, and the rest of our large family, thank you for all your support. This would not have been possible with such an amazing support system. Thank you also to my friends who have been there with me throughout my academic journey. Last but not least, thank you to my biggest supporter for all your patience, support, and love throughout this journey. Andres, you have always pushed me to accomplish all my goals and never let me give up. Words cannot express my gratitude.

This degree is an achievement I share with all of you. For without you, it would not have been possible.

Acknowledgments

I would like to thank Dr. Frisina for giving me the opportunity to learn and work in his laboratory at the Global Center for Hearing & Speech Research. Thank you for being a great PI and allowing me to complete my Ph.D. under your guidance. Thank you also for your encouragement with my presentations, I truly appreciated it.

I also want to express my appreciation to Drs. Ding and Zhu for teaching me laboratory procedures and having the patience in mentoring me throughout the completion of my Ph.D. project. Thank you for your support and for believing in me.

Thank you to Drs. Gallant, Jaroszeski, and Sanchez for being a part of my dissertation committee. I know it is not an easy task; thus, I am grateful for you all taking time out of your busy schedules to help me.

Lastly, I would like to thank all my lab mates for their help and friendships in and out of the lab. Lauren, Gbemi, Parveen, Mark, Tanika and Nicole – thank you.

Table of Contents

List of Tables

List of Figures

Abstract

Age-related hearing loss (ARHL), also known as presbycusis, is the number one communication disorder affecting our aged population. Connexin proteins are essential for intercellular communication throughout the human body. Mutations in connexin genes have been linked to human syndromic and nonsyndromic deafness; thus, we hypothesize changes in connexin gene and protein expression with age may be involved in the development of ARHL. In our current study, connexin mRNA gene expression for CBA/CaJ mice at different age points were examined and correlations were analyzed between the changes in gene expression and functional hearing measures, such as ABRs and DPOAEs. Moreover, we investigated potential treatment options for ARHL. Results showed significant downregulation of *Cx30* and *Cx43* gene expression in the stria vascularis (SV), and meaningful correlations between the degree of hearing loss and the changes in gene expression for both genes. Moreover, dose-dependent treatments utilizing cochlear cell lines showed that H_2O_2 oxidative stress significantly decreased gene and protein expression for *Cx30* and *Cx43*, while aldosterone hormone therapy significantly increased *Cx* expression. *In vivo* treatment of aging mice with aldosterone also revealed protective effects on connexin expression and ARHL. These findings support further quantitative analyses for measuring the exact effects of each treatment. Based on these functionally relevant findings, our goal is to determine more about the mechanisms related to connexin family gap junction protein expression changes during ARHL, and expand our knowledge of potential, innovative treatment options.

Chapter 1: Introduction

Hearing loss is a multifactorial sensory disorder that can be caused by a combination of genetics, loud noise, drugs, disease co-morbidities, and aging. Age-related hearing loss (ARHL), also known as presbycusis, affects over 10% of our worldwide population. [4] In the United States, over one-third of the population between the age of 65 and 74 are affected, and over half of those older than 75. [5] ARHL is a complex neurodegenerative disorder often depicted by having reduced sensitivity to sound, difficulty with sound localization and detection, speech perception deficits - particularly in noisy backgrounds, and slowed central processing of acoustic feature information. [6, 7] Clinically, ARHL can be detected first with hearing loss at higher frequencies that then progresses to lower frequencies with age. [8]

The perceptual effects of ARHL derive from biological changes in the auditory system. Our hearing system is comprised of the peripheral and central auditory systems. The peripheral auditory system includes the outer, middle, and inner ears. Housed in the inner ear is the vestibular peripheral neural organs and the cochlea. [9] The peripheral vestibular system provides inputs to the brain to support the ability to maintain balance, normal eye movements, and proper spatial orientation. [10] This system consists of the semicircular canals, the utricle, saccule, and vestibule that receive acoustic vibrations from the middle ear. [11] For the purposes of this dissertation, we will focus on the specialized sensory organ known as the cochlea. This fluid-filled cavity in the temporal bone works as a transducer that converts its fluid vibrations into the neural coding of sound signals; separating sounds into different frequency bands, before they are converted into

neural codes and sent to the central auditory system for perceptual processing, including speech and sound localization. [9, 11]

Anatomically, the cochlea is a spiral-shaped structure composed of several fluid-filled compartments and bony rigid walls. [2, 12] Two of these fluid-filled compartments are known as the scala tympani and scala vestibuli which are filled with a high sodium (Na^+) liquid called perilymph (similar to normal extracellular fluid), and a third compartment, the scala media, which is filled with an unusual high potassium (K^+) extracellular fluid called endolymph. [12] The specialized ionic composition of the endolymph is maintained by a structure found in the lateral wall of scala media called the stria vascularis (SV). [13] The SV generates the endocochlear potential and endolymph, resulting in an approximate +80mV potential. For this reason, the SV is often referred to as the "cochlear battery". [14] Cells in the SV have an abundance of mitochondria, indicating high metabolic activity. [9] It has been discovered that functional loss of the stria vascularis with aging leads to a reduction of the EP; thus, damaging stimulus transduction and coding performed by inner hair cells and the acoustic-mechanical amplification by outer hair cells. [15] The hair cells are located in the organ of Corti (OC) and are organized in an organized pattern on the basilar membrane. [16] So, the OC is responsible for the transduction of sound vibrations into neural signals, as nerve fibers from the auditory division of the 8^{th} cranial nerve are found within this organ, as they synapse with the hair cells. [12] Therefore, the connections between the OC and brain are provided by the spiral ganglion neurons (SGN). In sum, these neurons in conjunction with the hair cells in the OC transfer auditory signals from the basilar membrane to the cochlear nucleus in the brainstem. [17]

Critical to normal cochlear functioning, a dense network of gap junctions is found in the OC and cochlear supporting cells. Gap junctions, composed of protein units, are used for cochlear

intercellular communication; thus, they help regulate and move ions such as K+, electrolytes, secondary messengers, and metabolites between cells. [18, 19] Connexins (Cxs) are gap junction proteins that join to form complete gap junction ion channels and have been found in various types of cochlear tissue such as the SV, OC, and SGNs. [20-23] The structure of connexin proteins consists of six connexin subunits joining together to make a half channel called a connexon, and two connexons merge to make an intercellular connection (Figure 2). [23] There are 21 connexin isoforms found in the human body, and nine have been associated with hereditary disorders such as nonsyndromic and syndromic deafness, i.e., children born without normal gap junction proteins are profoundly deaf. [3, 18]

Mutations in genes encoding *Cx26* are responsible for up to 50% of all nonsyndromic sensorineural hearing loss, specifically a mutation known as 35delG. [24, 25] Moreover, connexin knockout mice also display an absence of the endocochlear potential, increase in reactive oxygen species (ROS), and cell degeneration. [26, 27] These proteins have been discovered in various areas in the cochlea including sensory and nonsensory epithelia, supporting cells and connective tissue cells. [21] It has been found that connexins are essential for the development of normal cochlear morphology, generation of the EP, K^+ recycling, and maturation of ribbon synapses that provide functional connections between inner hair cells and SGNs. [28] We hypothesize that connexins could be associated with ARHL firstly due to the fact that mutations in these proteins are known to cause hearing loss or deafness in young humans and animal models. Moreover, studies have found that cellular stress conditions similar to those seen in the aged cochlea, such as exposure to hydrogen peroxide (H_2O_2), affects connexin expression negatively. [29, 30]

Research on ARHL has led to a general consensus that the age-related degeneration of the cochlea is polygenic and multifactorial in etiology. [31] Examples of this are intrinsic factors such

as genetics and diseases, along with extrinsic factors like loud noise and drugs. The association between ARHL and connexins has yet to be established; however, it has been found that genetic mutations in connexin genes cause type two different types of hearing loss: nonsyndromic and syndromic hearing loss. [32] Due to their being an association between connexins and these types of hearing loss, our hypothesis that connexins may also be linked to ARHL is logical, as they play an important role in the maintenance of hearing function. Proposed mechanisms for how mutations of a single connexin gene can cause deafness are illustrated in Figure 3. The mechanisms explained in this figure may also be applied to connexins and ARHL, as the functions that are affected by mutations in connexin genes may also be altered during ARHL. Additionally, another potential link between ARHL and connexins is that aging in other areas of the body alters connexin expression. For example, *Cx43* expression is reduced in the heart as aging occurs, and this contributes to the decrease in conduction velocity in older hearts. [33] Mechanisms observed in the cochlea that are associated with aging, such as increases in ROS, changes in potassium channels, and increased inflammation have also been shown to affect gap junction channels. [34-39]

One potassium channel that plays an essential role in the cochlea is the inward rectifying K^+ channel, Kir4.1. Kir4.1, encoded by the KCNJ10 gene, is a part of the K^+ transport channels called Kir which consists of 7 subfamilies. [40] In the inner ear, Kir4.1 is involved in the maintenance of SGN excitation, generating high K^+ concentration in the endolymph and the positive endocochlear potential, and is found in the supporting cells in the OC. [41, 42] The SV, which is responsible for production and maintenance of the endocochlear potential is composed of three distinct cell layers: marginal, intermediate, and basal. Within these layers there is an extracellular space named the intrastrial space (IS) which is in between the basolateral membrane

of the marginal and apical membrane of the intermediate cells. [43, 44] In the apical membrane of the intermediate cells, Kir4.1 channels are responsible for K^+ permeability. They work in conjunction with gap junctions that connect the intermediate cells with the basal cells in the spiral ligament to produce the endocochlear potential. [45, 46] In the SGN, Kir4.1 channels have been hypothesized to absorb K^+ ions that are expelled from SGNs during excitation, into satellite glial cells. [47] Sensorineural deafness has been attributed to mutations in Kir4.1 genes. [48, 49] Moreover, Kir4.1 knockout mice also display a deficiency of K^+ in scala media, nonexistence of the endocochlear potential, collapse of Reissner's membrane, SGN demyelination and degeneration of hair cells. [50-52] Thus, causing the knockout mice to be deaf.

Aldosterone is a steroid hormone secreted from the adrenal cortex that has been shown to have protective effects against hearing loss. [53-55] Pre-clinical studies have shown that aldosterone is effective in slowing down the progression of ARHL, lowering/improving hearing thresholds, and preventing apoptosis in spiral ganglion neurons. [54, 56, 57] This naturally occurring hormone is a good candidate for treatment of ARHL as it seems to be relatively safe when serum levels are well controlled; however, a main potential side-effect is hypertension if not regulated carefully. Aldosterone is highly involved in the regulation of blood pressure due to its role in maintaining the levels of salt and water in the body, which moderates blood volume. Our lab, including Halonen et al. (2016), administered aldosterone to CBA/CaJ mice and measured their blood pressure to ensure there was no elevation. They found the mean systolic (~120 mm Hg) and diastolic (~85 mm Hg) levels remained stable throughout their 4-month study compared to the baseline measurements. [54] Aldosterone has also been found to regulate expression of potassium channels, such as Kir4.1 (KCNJ10) in other areas of the body, such as the retina. [39] If our hypothesis that potassium channels are related to connexin protein expression, aldosterone's

therapeutic effect may potentially involve counteracting age-linked declines in connexin protein expression.

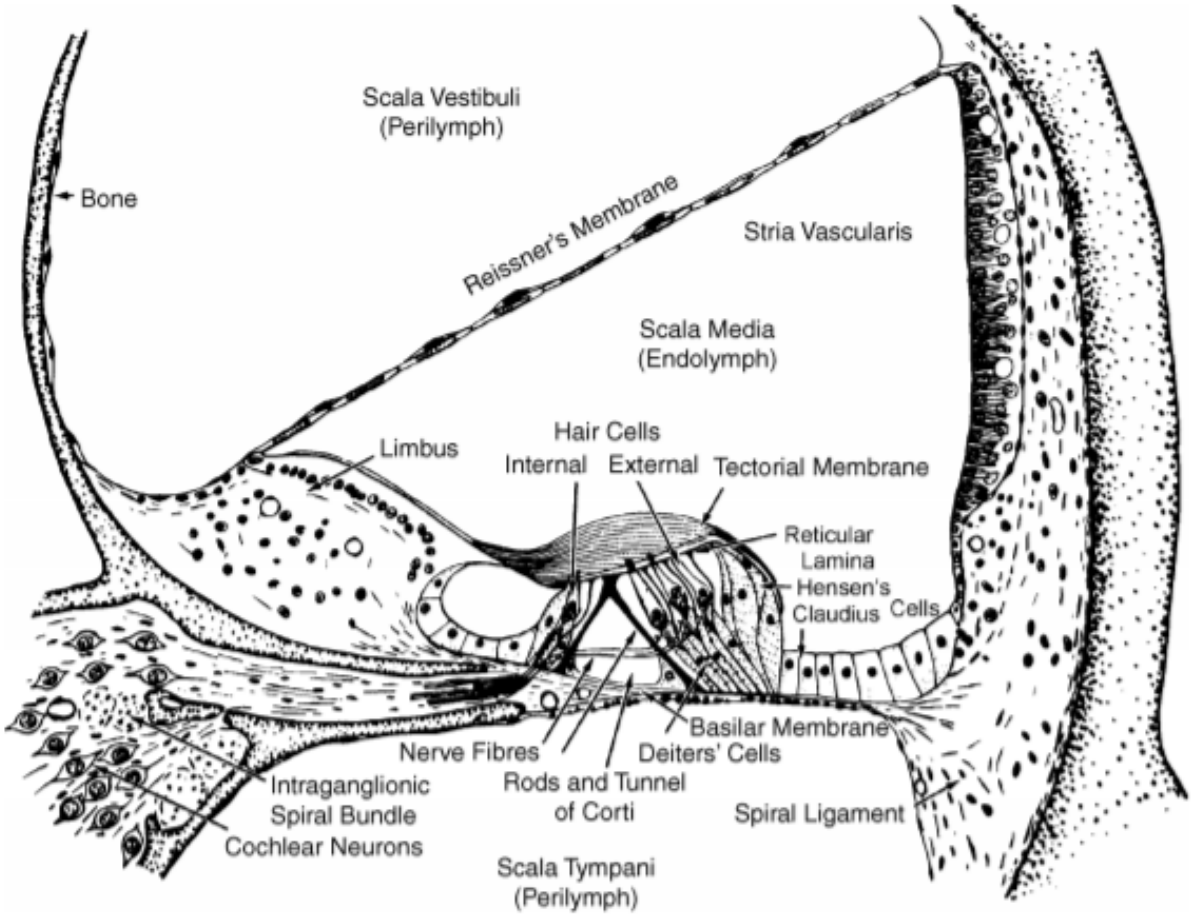

Figure 1. *A cross-section of a guinea pig's cochlea.* The three compartments (scala vestibuli, scala media, and scala tympani) along with the organ of Corti and the stria vascularis are displayed. Figure is from Chapter 1, Figure 1.5 from B.C.J. Moore book. [2]

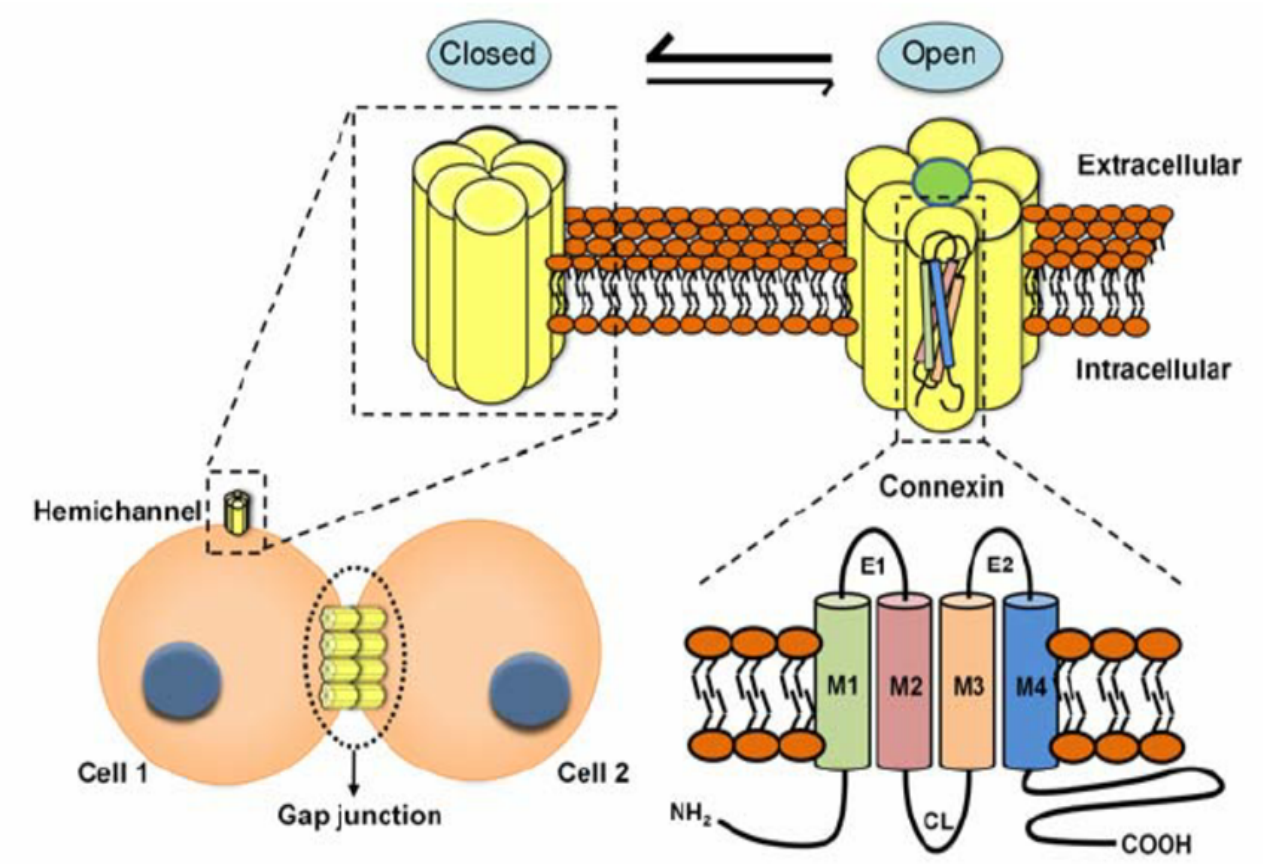

Figure 2. *The basic structures of connexins and a visual of how connexins connect to form a gap junction between two cells*. At the bottom right, the composition of a single connexon which contains: 4 domains interwoven in the membrane (M1-M4), 2 extracellular loops (E1 and E2) and 1 cytoplasmic loop (CL), along with an amino (-NH 2) and carboxy (-COOH) terminal tail that are located inside the cell, is shown. This figure is from Orellana et al. (2011) [1]

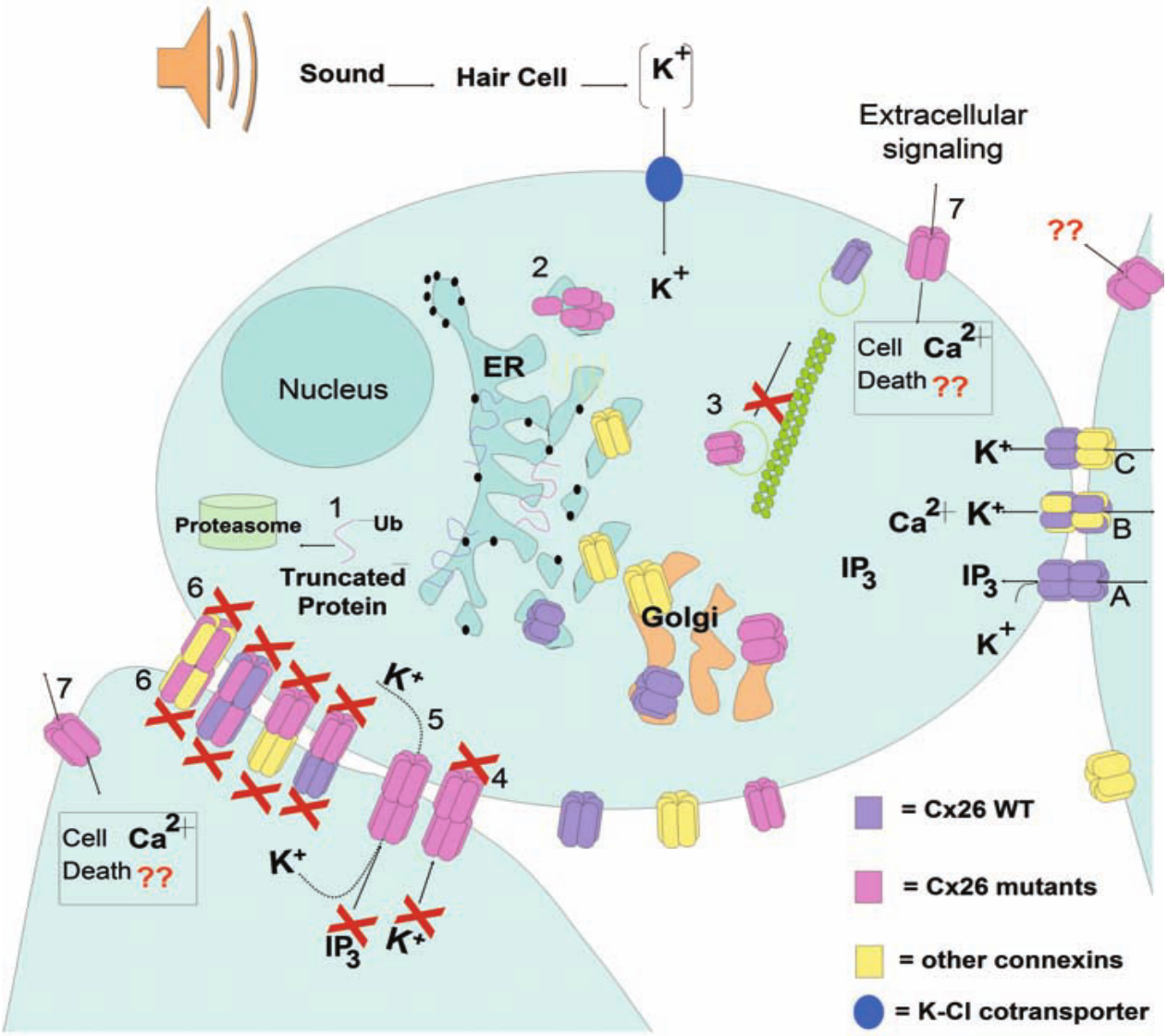

Figure 3. *Mechanisms of deafness-associated Cx26 mutations*. (A) Cx26 homomeric channels are permeable to ions and molecules such as K+ and IP3. Homomeric Cx30 channels are highly permeable to K+ but lower permeability to IP3. (B) Heteromeric Cx26–Cx30 channel. (C) Heterotypic Cx26 and Cx30 channel. Cx26 mutations may produce: 1. Shortened protein connexin, 2. Defects halting the formation of hemichannels, 3. The path of the hemichannel being altered, not allowing it to get to the plasma membrane, 4. Nonfunctional channels (closed channels halting the transportation of ions and molecules), 5. Working channels permeable to ions but not bigger molecules such as IP3, 6. Mutant Cx26 that can produce nonfunctional heteromeric channels with normal connexin hemichannels. 7. Abnormal hemichannels in the plasma membrane that increase permeability, which can cause loss of intracellular metabolites (i.e., ATP) or increase intracellular calcium concentrations, which can lead to cell death. [3]

Chapter 2: Methods

This portion of the study utilized methodologies based upon Frisina and colleagues. [58-60]

2.1 Animal Model

CBA/CaJ mice are used because they lose their hearing progressively with age; therefore, making them an excellent model for human ARHL. The CBA/CaJ mouse breeding pairs were bought from Jackson Laboratories (Bar Harbor, ME) and bred in-house following institutional protocols. All procedures were approved by the University of Rochester and University of South Florida Vivariums and IACUC and were compliant with NIH policies. A total of 86 mice were used for different sets of experiments: the Affymetrix GeneChip analysis, aldosterone study, quantitative polymerase chain reaction (qPCR), and confocal microscopy.

2.1.1 Affymetrix GeneChip

For the Affymetrix GeneChip analysis, 40 of the mice were classified into four groups according to age and degree of hearing. The groups were divided as followed: young adult with good hearing (YA, N=8, 3.5±0.4 months), middle-aged (MA, N=17, 12.3±1.3 months), mild presbycusis (MP, N=9, 27.7±3.4 months), and severe presbycusis (SP, N=6, 30.6±1.9 months). The YA group was used as the baseline group for the gene expression analysis (i.e., for calculating fold changes). The other 20 mice used for the age comparison study utilizing RT-qPCR were split into two groups: young adult (Y, N=10, 3±1.5 months) and old (O, N=10, 28±2.5 months). All PCR animal protocols were approved by the University of South Florida Vivarium and Institutional Animal Care and Use Committee (IACUC).

2.1.2 Aldosterone Animals

Aldosterone treatment was conducted by Frisina et al. (2016). [56] Eighteen CBA/CaJ mice (15-18 months at baseline) were assigned randomly to control (n=10) or treated groups (n=8). The treated mice received a custom d-aldosterone pellet (0.0016 mg/day, 120-day release, Innovative Research of America, Sarasota, FL) and the control group received a saline placebo pellet. The pellets were implanted subcutaneous behind the shoulders while the mice were anesthetized with ketamine/xylazine (120 and 10mg/kg). A baseline ABR recording was done at prior receiving the pellets and two subsequent recordings were done at 2 and 4 months. At the conclusion of the treatment period, the mice were sacrificed by decapitation and their cochleae were dissected and stored in -80^{o}C for future experiments. A subset of these cochleae 3 treated, were collected for RT-qPCR and confocal microscopy experiments done in this study to be compared with control, young (n=3, 3±1 months) and old (n=3, 23±1.5 months) mice.

2.1.3 RT-qPCR Animals

Young (n=10, 3±1 months) and old (n=12, 27±3months) were obtained for RT-qPCR aging experiments.

2.2 Hearing Assessments

2.2.1 Auditory Brainstem Responses (ABR) and ABR Gap-In-Noise (GIN)

CBA/CaJ mice were anaesthetized with a mixture of ketamine/xylazine (120 and 10mg/kg body weight, respectively, via an intraperitoneal injection) before auditory examinations and kept on a heating pad inside a soundproof acoustic chamber (IAC lined with Sonex) to maintain their body temperature (37°C) throughout the experiments. Acoustic stimuli were synthesized digitally using the System III Tucker-Davis Technology (TDT, Alachua, FL) signal-processing platform. The stimuli were then attenuated and filtered (low-pass cutoff at 5kHz). Stimulus sounds were

presented through an electrostatic speaker (TDT EC1) connected to the external ear canal by 4cm tubes, that is via a calibrated, closed system. A ¼ inch B&K microphone (Type 4938, Bruel & Kjaer, Naerum, Denmark) attached to a .1cm^3 coupler was used to calibrate the TDT system daily. The mice were placed on a heating pad inside a soundproof booth. Three platinum needle electrodes were subcutaneously inserted at the vertex (non-inverted and in the mastoid area muscle of the ipsilateral (testing) side (inverted), with a ground electrode being inserted into the muscle posterior of the contralateral pinna to record the ABR responses. These electrodes were connected to a bioamp head stage (HS4 Fiber Optic, TDT). For ABR threshold experiments, the mice were presented with tone pips of 3, 6, 12, 16, 20, 24, 32, and 48 kHz. a wide band noise (WBN) stimulus, having a bandwidth from 0 to 48kHz, was also used. The duration for each ABR stimulus was 5ms, presented at a rate of 21 bursts/second. For ABR GIN, a silent gap was inserted in the center of two WBN bursts, NB1 and NB2, at 80dB SPL, each with a repetition rate of 21/sec, duration of 25ms and rise-fall times of 0.5ms, and each averaged response was obtained from 100 stimulus presentation and then duplicated with another 100 repetitions. Gap durations were 0, 1, 2, 4, 8, 16, 32, and 64ms. Responses were recorded using BioSig (TDT) and duplicated for each gap duration tested. The time span for each ABR GIN audiogram response window was 150ms. [61]

2.2.2 Distortion-Product Otoacoustic Emissions (DPOAE)

CBA/CaJ mice were placed in exact same conditions as ABR experiments: anaesthetized with a mixture of ketamine/xylazine (120 and 10mg/kg body weight, respectively, via an intraperitoneal injection) before electrophysiology experiments and placed inside a soundproof booth (IAC lined with Sonex) on a heating pad to maintain body temperature. Before recording, the stimulus probe and microphone coupler were placed in the test ear near the tympanic membrane with the aid of an operating stereoscope. Ipsilateral acoustic stimulation and simultaneous

measurement of DPOAEs were accomplished with a TDT BioSig System III. Stimuli were digitally synthesized at 200kHz using SigGen software with the ratio of f2/f1 constant at 1.25, and L1 = 65 dB and L2 = 50 dB SPL, as calibrated in a 0.1cm^3 coupler simulating the mouse ear canal. After synthesis, f1 and f2 were passed through an RP2.1 D/A converter to PA5 programmable attenuators. Following attenuation, the signals went to ED1 speaker drivers which fed into the EC1 electrostatic loudspeakers coupled to the ear canal via short flexible tubes with rigid plastic tapering tips. For DPOAE measurements, the resulting ear canal sound pressure was recorded with an ER10B+ low noise microphone (gain 20x) and probe Etymotic, Elk Grove Village, IL) housed in the same coupler as the f1 and f2 speakers. The output of the ER10B+ amplifier was inputted to an MA3 microphone amplifier, the output of which wen tot an RP2.1 A/D converter for sampling at 200kHz. A fast Fourier transform (FFT) was performed on the resultant waveform. The magnitude of f1, f2, the 2f1-f2 distortion product, and the noise floor of the frequency bins surrounding the 2f1-f2 component were measured from the FFT. The procedure was repeated for geometric mean frequencies ranging from 5.6-44.8kHz (8 frequencies/octave) to assess adequately the neuroethological functional range of mouse hearing. Duration of the testing was approximately one hour per animal. [62]

2.3 GeneChip Data Access

The entire microarray probe-set from each GeneChip M430A (Affymetrix Inc., Santa Clara, CA) and individual CBA mouse phenotypic (hearing measures) data have been submitted to the GEO-NCBI database and have been approved with the following Series reference #: GSE GSE49543. These GeneChip data can be accessed via, http://www.ncbi.nlm.nih.gov/geo/query/acc.cgi?acc=GSE49543. The probe-sets used were

derived from the above GEO-NCBI accession number GSE49543. All steps were conducted according to the MIAME (Minimum Information About a Microarray Experiment) checklist. [60]

2.4 Cell Culture and Treatments

SV-k1 epithelial and HEI-OC1 cells were cultured in permissive conditions [(33ºC, 10% CO_2, Dulbecco's modified Eagle's medium (DMEM) supplemented with 10% fetal calf serum (FCS)]. At least 24hr before treatment, the cells transferred to grow in the non-permissive condition (39ºC, 5% CO_2, DMEM with 5% FCS) were split into 100mm plates (Falcon). Experiments were performed at 70-80% confluence. All treatment started after the switch from permissive to non-permissive condition. The cells were split into 5 groups for each treatment, with each group receiving different dosages of the treatment. For the hydrogen peroxide (H_2O_2) treatment, the groups included: Control, 10μM, 40μM, 80μM, 100μM, and 120μM. The aldosterone treatment group was divided into: Control, 1nM, 10nM, 1μM, 5μM. A combination treatment was conducted by treating the cells with 100μM H_2O_2 for four hours and then 1μM of aldosterone was added. The dosages chosen were determined from previous studies. [63-65] After 24hr treatment, the adherent cells were scraped off the plates using a cold plastic cell scraper, then gently transferred into an Eppendorf tube. The collected cells were stored in -80ºC until future use. [66, 67]

2.5 Real-time Quantitative RT-PCR

This procedure has been previously described by Ding et al. [66] SV tissue samples extracted from the cochlea of mice from the aging and aldosterone studies, and the cells collected were used for the following experiment. RNA from mouse samples and cells were extracted using the RNAeasy Mini Kit (Qiagen, Valencia, CA). Samples were vortexed for 1 minute to shear genomic DNA before loading onto the RNeasy columns, and then eluted in a minimum of 30mL

and a maximum volume of 2x50 mL RNAsefree water. RNA obtained with the procedure was essentially free of genomic DNA. 50ng of RNA was then used to synthesize 20uL of complimentary DNA (cDNA) using an iScript cDNA kit (Bio-Rad Laboratories; Hercules, CA). Once the sample mixtures were made, they were incubated for 2 min at 94ºC (initial denaturation), 15 s at 94ºC (denaturation), 30s at 55ºC (annealing), 1 min at 68ºC (extension), and 5 min at 68ºC (final elongation). The denaturation, annealing, and extension steps were repeated for 35 cycles. Primer sequences used to detect the genes were as follows: Cx30 Forward: 5'-GAAGTGTGGGGTGATGAGCAGGAG-3', Cx30 Reverse: 5'-CGTGGACTGCTTCATTTCGAGGCC-3', Cx43 Forward: 5'-CTCCTCCTGGGTACAAGCTG-3', and Cx43 Reverse: 5'-GTTCGATTTTGCTCTGCGCT-3'.

Primer specificity was performed as previously described. [66] Triplet repeated quantitative PCR (qPCR) experiments were executed by creating a master mix using the aforementioned primers, SsoFast™ Evagreen (Bio-Rad, Hercules, CA), RNase-free water and the cDNA samples. The samples were then placed in a Analytik Jena qTOWER^3 (Thuringia, Germany) to generate a quantitative analysis of the genes expressed in both the SV-k1 cells and in vivo SV tissue samples. Each experiment always included a no-sample negative control (NTC) to ensure no contamination and that the primers were working. A parallel PCR reaction was performed using glyceraldehyde 3-phosphate dehydrogenase (GAPDH)-specific primer as the housekeeping gene. Calculations of gene expression were performed with the 2ΔΔCT method. [66-68]

2.6 Western Blot

Cell lysates were prepared in radioimmunoprecipitation assay buffer (RIPA, Pierce #89901, Thermo Scientific, Waltham, MA) with protease inhibitor cocktail (#78430, Thermo

Scientific, Rockford, IL). Cells were homogenized in buffer, followed by centrifugation at 13,000 rpm for 10 min at 4ºC. Supernatants were subjected to western blot analysis by loading 30ug protein per lane, after the protein concentrations were determined utilizing the Bradford protein assay. Proteins were fractionated by SDS-PAGE gel electrophoresis and transferred to a PVDF blotting membrane overnight at 30mV. The membrane was then washed 3 times with phosphate-buffered saline with Tween 20 (PBS-T) for 15 min each wash and blocked using 5% non-fat milk for 1 hr. The blot was then washed PBS-T 3x15 min and then incubated with primary antibodies overnight at 4ºC. The membrane was washed with PBS-T 3x15min and incubated with the secondary antibody for 2 hrs. After a final 3x15min with PBS-T, the membrane was placed in 20X LumiGLO Reagent and 20X Peroxide (#7003, Cell Signaling, Danvers, MA) for 1 min before imaging.

The primary antibodies used included: Cx30 (1:250, #71-2200, Invitrogen), Cx43 (1:250, ab11370, Abcam), β-actin (1:1000, Cell Signaling, Danvers, MA), and GAPDH (1:1000, ab9485, Abcam). The secondary antibody was horseradish peroxidase-conjugated goat anti-rabbit IgG (1:2000; Cell Signaling). [66]

2.7 Immunohistochemistry

2.7.1 Preparation of Samples

Six cochleae collected from our aldosterone study, (Frisina et al. 2016) control old, n=3, 22-24 months; aldosterone-treated, n=3, 22-24 months) and three young adult mice cochlea (3-4 months) were stored in -80°C prior to this experiment. [56] Prior to being stored, the cochleae were placed in 10mL of fresh 4% paraformaldehyde (Thermo Scientific, Rockford, IL) in PBS (0.1M, pH 7.6) in 4°C overnight. After fixation, the samples were washed 3x10min in PBS and then decalcified in 20mL 10% EDTA (ethylenediaminetetraacetic acid, Fisher Scientific,

Pittsburgh, PA) in PBS at 4°C. The decalcification took approximately 1 week to complete; however, the cochleae were checked daily. Following this, the cochleae were washed 3x10min in PBS, and then transferred into 10% and 20% sucrose (Acros, Geel, Belgium) in PBS for 2 hours. The samples were then placed in 30% sucrose in PBS overnight at 4°C. Lastly, the cochleae were embedded into degassed OCT (Tissue-Tek, Torrance, CA) at 4°C, oriented into a cryomold (Tissue-Tek) with degassed OCT for 1 hour, and frozen at -80°C. Cryosectioning was done at 5μm/section and then mounted on glass slides.

2.7.2 Cx30, Cx43 and Kir4.1 Staining

Slides were rinsed with 1xPBS + .1% Triton X-100 3x5 minutes. Next the tissues were placed in a damp black box and incubated in blocking solution (10% goat serum + 0.1% Triton X-100 + 1% BSA in PBS) for 1hr. If mouse-on-mouse staining was going to be done, a subsequent block was performed utilizing anti-mouse-IgG blocking reagent (Vector Laboratories, Newark, CA, Cat. No. MKB-2213). Afterwards, the samples were incubated with the primary antibodies at 4^{o}C overnight. The next day, the samples were washed 3x15 min with PBS and incubated with the secondary antibodies for 1hr. The secondary antibodies were washed out with DI H_2O, 3x10 min). The samples were then mounted onto slides with mounting medium (Prolong^{TM} Gold antifade reagent with DAPI, 1:1000) for 2-5 minutes and observed using a confocal laser scanning microscope (Nikon Corporation, Tokyo, Japan).

The primary antibodies used were Cx30 anti-rabbit (1:100, #712200, Invitrogen), Cx43 anti-mouse (1:100, #13-8300, Invitrogen), and Kir4.1 (1:200, #12503-1-AP, Proteintech). The secondary antibodies used were Alexa Fluor 488 goat anti-rabbit IgG, Alexa Fluor 594 goat anti-mouse IgG, and goat anti-rabbit Alexa Fluor 594 (1:1000, ThermoFisher Scientific, Waltham, MA).

2.7.3 Laser Scanning Confocal Imaging

Confocal imaging was done utilizing a Nikon A1 HD25 Multi-Photon & Laser Scanning Confocal combined with a Nikon Eclipse Ti2 inverted microscope. Images were taken at 10X and 20X via excitation at 405, 488, and 594 nm wavelength for DAPI, Cx30, Cx43, and Kir4.1 at a scan speed of 0.5 frames/second. Z-stack images were taken at 0.5µM steps at digital zoom levels of 4.21 and 8.96. Each stack was exported into individual images used for fluorescence intensity analysis and cell counting of the apex, middle, and basal regions for each animal cochlea.

2.8 Statistical Analysis

2.8.1 GeneChip Expression Analysis

The data from the GeneChip array was imported into Microsoft Excel showing the raw gene expression level values. The gene expressions for each sample were converted into signal log ratio (SLR) to determine the difference in expression of the studied gene in that sample from the mean expression of that gene in all samples from the young adult mice. A signal log ratio of 1.0 indicates an increase of the transcript level by 2-fold and −1.0 indicates a decrease by 2-fold. A signal log ratio of zero indicates no change.

For the six connexin GeneChip probes, the ROUT method (Q=1%) was applied to find any outliers within the dataset. Then the raw gene expression was converted into SLR. One-way Analysis of Variance (ANOVA) (95% confidence limit) was used to compare between the signal log ratio values of the different subject groups. In addition, fold changes of all samples were calculated from signal log ratios using the following equations:

$$Fold\ Change = 2^{signal\ \log ratio}\ if\ signal \log ratio \geq 0$$

$$or\ (-1)x2\text{^}((-signal \log ratio))\ if\ signal \log\ ratio < 0$$

Linear regression comparing the changes in gene expression and hearing ability was also conducted. These statistical tests were conducted using GraphPad Prism 6.0 (GraphPad Software, La Jolla, CA).

2.8.2 Real Time qPCR Analysis

The threshold cycle (C_T) values were measured to detect the threshold of each of four significant genes of interest and GAPDH gene in all samples. Each sample was measured in triplicate and normalized to the reference control GAPDH gene expression. The C_T value of each well was determined and the average of the three wells of each sample was calculated. For samples that showed no expression of the test gene, the value of minimum expression was used for statistical analysis.

Delta $_{CT}$ (ΔC_T) for test gene of each sample was calculated using the equation:

$$\Delta C_T = C_T TestGene - C_T GAPDH$$

Delta delta C_T ($\Delta\Delta C_T$) was calculated using the following equation:

$$\Delta\Delta C_T = \Delta C_T SampleAverage - \Delta C_T YoungGroup$$

Lastly, the fold change in the test gene expression was calculated from the formula:

$$Fold\ Change = 2^{(-\Delta\Delta C_T)}\ if\ \Delta\Delta C_T \leq 0\ or\ \frac{-1}{2^{(-\Delta\Delta C_T)}}\ if\ \Delta\Delta C_T > 0$$

A statistical evaluation of real time PCR results was performed using a one-way ANOVA one-way ANOVA followed by Bonferroni *post hoc* tests to compare between the gene expression values for the young adult age, middle age, old age mild presbycusis, and old age severe presbycusis groups from the GeneChip (N=40 mice), along with comparing the young and old animals from the PCR aging study (N=20 mice). For the cell treatment experiments, t-test were utilized to compare the difference in gene expression values between the different dosages used.

For the two significantly different genes on GeneChip and/or qPCR, linear regression analyses were employed to find correlations between the signal log ratio values or fold changes, and the functional hearing measurements (ABRs, DPOAEs). These measurements were the distortion product otoacoustic emission (DPOAE) amplitudes at low frequencies (5.6 kHz to 14.5 kHz), mid frequencies (15.8 kHz to 29.0 kHz) and high frequencies (31.6 kHz to 44.8 kHz), in addition to auditory brainstem response thresholds (ABR) at 3, 6, 12, 24, 32 and 48 kHz. Microsoft Excel and GraphPad Prism 9.0 software (GraphPad, La Jolla, CA) were used to do the conversions and calculate the one-way ANOVA and the linear regression statistics. [60]

2.8.3 Densitometric Analysis

Images from Analytic Jena UVP Chem Studio SA2 were imported to NIH ImageJ software for the densitometry analysis and the data are reported as mean±SD. Using ImageJ, the image was saved in a TIFF format and processed using the Process > Subtract Background command to reduce background noise. The “rectangle” tool from ImageJ was used to frame the largest band for each row. For each protein band across the lanes, each single region of interest was defined using the same frame as the largest band. With the same frame as the protein (row) a background measurement was taken. This procedure was done for the other rows or loading controls and the measurements for the bands and their backgrounds were exported to Excel. The pixel density for all data (bands/controls + their backgrounds) were inverted and put in new columns. The inverted values are expressed as 255 – X, where X is the value recorded by ImageJ. For the protein bands and loading controls, the net values were expressed by deducting the inverted background from the inverted band value. When the net bands and loading controls were calculated as the final step, a ratio of a net band value over the net loading control of that lane was calculated. The final relative quantification values are the ratio of the net band to the net loading control. Differences were

analyzed with a one-way or two-way ANOVA as appropriate, with a two-way ANOVA followed by Bonferroni *post hoc* tests and corrected for multiple comparisons, with $p<0.05$ considered significant, using GraphPad Prism 9.0. [63, 66]

2.8.4 Confocal Analysis

On NIS-Elements Advanced Research (Nikon Instruments Inc., Melville, NY), each image was imported to analyze the fluorescence intensity of each protein and count the cells. First a region of interest (ROI) was selected for each region of the cochlea - SV, OC, SGN. Each region's ROI size was determined by ensure that critical regions were included, i.e., for the OC, hair cells must be in the ROI. The sizes of the ROIs were consistent in size for all three turns and regions chosen to measure. Cell counting was done utilizing the software's automated measurement counter identifying DAPI, which labels DNA within the nucleus of each cell. Parameters for the counting were adjusted for the intensity ranges of the 405 (blue) channel, separation, and size to ensure accurate cell counting. The fluorescence intensity was achieved by subtracting out the background of the image in the DAPI channel and the NIS-Elements Advanced Research software quantified the mean fluorescence intensity for each wavelength [405 (blue), 488 (green), and 594 (red)]. The intensity averages of each animal were added up within their respective group (young, old, and aldosterone-treated) and analyzed for significant differences between each group utilizing GraphPad Prism 9.0. Cell differences between the groups were also compared in the GraphPad Prism 9.0 software. The statistical analysis included a one-way or two-way ANOVA, as appropriate, followed by Bonferroni *post hoc* tests and corrected for multiple comparisons, with $p>0.05$ considered significant.

Chapter 3: Results

3.1 Expression of Connexin Genes Change With Age

3.1.1 GeneChip Analysis

3.1.1.1 Auditory Tests Confirm Progression of ARHL Between Animal Subject Groups

CBA/CaJ mice (N=40) were subjected to a series of auditory tests, ABRs and DPOAEs, and classified into groups based on age and degree of hearing loss. The four resulting groups included: Young Adult (YA) with good hearing (N=8, 4 males and 4 females, age: 3.5±0.4 months), Middle-Aged (MA) with good hearing (N=17, 8 males and 9 females, age: 12.3±1.3 months), old with Mild/Moderate Presbycusis (MP, N=9, 4 males and 5 females, age: 27.7±3.4 months), and old with Severe Presbycusis (SP, N=6, 2 males and 4 females, age: 30.6±1.9 months). [39, 40] The following data confirms that age-related hearing loss was occurring across the four age groups (Figure 4).

3.1.1.2 Downregulation of Connexin Genes Revealed in GeneChip Analysis

Twelve connexin (*Cx)* gene probes were identified in the set of over 22,000 CBA/CaJ mouse gene probes in our Affymetrix M430A GeneChip array. The gene expression levels were first tested for outliers using the ROUT method (Q=1%) using GraphPad Prism. Then the remaining gene expression levels for each sample were converted into fold change and signal log ratio (SLR) to determine the difference in expression of the YA mice compared to the other groups. Comparisons of the fold changes and SLRs between the MA, MP, and SP groups revealed statistically significant fold changes in *Cx30* (probe set ID: 1448397_at) and *Cx43* (probe set ID: 1415800_at) gene expression levels (Figure 5). The average fold change values for these genes

along with the one-way ANOVA results are summarized in Table 1. These gene expression changes for the two *Cx* genes were then subjected to further validation with RTqPCR.

3.1.1.3 Correlation Between Hearing Measurements and Gene Expression Levels

Linear regression tests were used to analyze if there were any correlations between the auditory ability of the animals and the gene expression levels for *Cx30* and *Cx43*. There was a significant correlation found for *Cx30* in relation to the ABR thresholds at all frequencies versus the fold change values (Figure 6A-B). No significant correlations were found between *Cx43* fold change and ABR thresholds; however, there was near significant correlations (p=0.11 and 0.07 for 6kHz and 3kHz, respectively), see Figure 6C. There was a significant correlation found between *Cx30* fold change values and DPOAE amplitudes at low- and mid-frequencies (p=0.03 and 0.02, respectively). There were no statistically significant correlations between *Cx43* gene expression and DPOAE amplitudes (Figure 7). Figure 8 displays correlations between *Cx30* and *Cx43* SLR gene expression and ABR thresholds.

3.1.2 RT-qPCR

3.1.2.1 Verifying ARHL Is Present, Comparing Young Adult and Old Mice

Two groups of CBA/CaJ mice were separated by age and hearing ability. The young adults (N=5, 3±1.5 months) and old (N=5, 28.2±2.5 months) groups underwent ABRs and DPOAE recordings to measure age-related hearing loss (ARHL) changes. The animal model audiological data collected are shown in Figure 9. These hearing tests demonstrated a significant increase in thresholds and decrease in DPOAE amplitudes for old mice relative to the young adults.

3.1.2.2 RT-qPCR Showed Gene Expression Levels of Cxs Change with Age

The validation of the GeneChip results were positive for *Cx30:* gene expression in the OC and SV of cochlea was significantly *downregulated* with age. *Cx43 PCR* results were also

consistent with the GeneChip results. Figure 10 shows the quantitative results comparing the fold changes of the young adult and old animals with the fold changes obtained from the GeneChip. From the GeneChip, the old animal group consisted of combined data from the mild presbycusis and severe presbycusis subjects.

RT-qPCR experiments were done after separating the stria vascularis (SV) and organ of Corti (OC). The results from these separate experiments show a significant downregulation in the SV for both, *Cx30* and *Cx43*, and a trend of upregulation in the OC for both gene expressions (Figure 11).

3.1.2.3 Protein Expression of Cxs Decreases with Age

Images taken using confocal laser microscopy show the downregulation of *Cx30* and *Cx43* protein expression between young adult and old mice. Figures 12 and 13 show images representative of these findings while Figure 14 provides the quantified results showing the differences in fluorescence intensity of the antibody labeling. The downregulation of both *Cx* proteins was found to be statistically significant in the OC of the middle and basal turns (Figure 14B) and in the SV in the apex of the cochlea (Figure 14A). Cell counts included all cells detected via DAPI staining. In Figure 14, panels G-I, cell loss data consistent with the aging cochlea is observed.

3.2 Cells Treated with Aldosterone and Hydrogen Peroxide Modulate Cx Expression

3.2.1 Gene Expression of Cx30 and Cx43 Is Protected Following Aldosterone Treatment

After treatment with hydrogen peroxide (H_2O_2, to simulate oxidative stress that occurs with age) and aldosterone for 24 hours, SV-k1 cells were collected and analyzed in triplicate RT-qPCR experiments. Figure 15 shows the quantitative results from these cell line treatment experiments. The gene expression of *Cx30* and *Cx43* were found to downregulate following H_2O_2 treatment

alone at multiple doses: 10μM, 40μM, 80μM, 100μM, and 120μM. On the other hand, *Cx30* gene expression increased in the SV-k1 cell line following aldosterone treatment at these doses: 1μM, 5μM, and 10μM. Cx43 showed very little change in expression for aldosterone treatments. Following a combination treatment of H_2O_2 (100μM) and aldosterone (1μM), there was a significant upregulation in *Cx30* and *Cx43* gene expression.

3.2.2 RT-qPCR Results Are Mirrored in Western Blot Experiments

Utilizing the same experimental conditions as the RT-qPCR cell treatment conditions, SV-k1 and HEI-OC1 cells were treated and collected to analyze the protein expression changes of *Cx30* and *Cx43*. The following triplicate experiment results mirror those obtained for the RT-qPCR findings. The densitometry analysis showed that *Cx30* protein levels decreased following H_2O_2 treatment alone for 24 hours at multiple doses; however, the protein expression increased after being treated with aldosterone (Figure 16). These results validate that aldosterone has a protective effect on *Cx30* expression, while H_2O_2 can be used to mimic aging to a first approximation.

3.3 Aldosterone Treatment Provides Protective Effects against ARHL

3.3.1 Hearing Function Is Improved Following Systemic Aldosterone Treatment

ABR tests were conducted on CBA/CaJ mice (N=6, 22-24 months). These mice were split evenly into two groups: control and treated. (Frisina et al., 2016) The ABR threshold shifts of the control mice were found to be significantly higher than those of the aldosterone-treated mice (Figure 17). A negative shift in the thresholds indicate that there was improved hearing in the mice which was observed at 12, 24, 32, and 36kHz in the aldosterone-treated animals. The positive shifts, as seen in the control mice, are characteristic of ARHL. Overall, ABR thresholds recorded from aldosterone-treated mice showed consistent threshold levels throughout the four months

while the control mice who showed age-related hearing loss elevations. These data indicate that aldosterone treatment provides a therapeutic effect on auditory brainstem responses for aging mice.

3.3.2 Aldosterone Treatment Does Not Significantly Alter Cx Gene Expression for In vivo Samples

A quantitative analysis of the gene expression of *Cx30* and *Cx43* was performed utilizing cochlear tissue samples collected from the CBA/CaJ mice after the four-month-long treatment (Frisina et al. 2016). Figure 18 shows that the samples from the aldosterone-treated mice did not display any marked gene expression changes compared to the control animals.

3.3.3 Confocal Imaging Shows Upregulation of Cx Proteins in Mice Treated with Aldosterone

Cochlear samples collected from the CBA/CaJ mice were later stained to analyze the protein expression of *Cx30* and *Cx43* utilizing confocal laser scanning microscopy. The apex, middle, and basal regions of the mouse cochlea were analyzed; moreover, within each region the SV, OC, and spiral ganglion neurons (SGN) were examined (Figure 23). We found that the level of protein expression for both *Cx* proteins was lower in the SV, OC, and SGN in old (22-24 months) mice compared to adult young mice (3 month) in all three turns of the cochlea. At the same time, protective effects of aldosterone were seen in the cochleae of mice that were treated with aldosterone (22-24 months). These mice exhibited significantly higher *Cx30* protein expression compared to both young adult and old mice. The expression of *Cx43* was also higher compared to young adult and old mice, except in the OC. In the OC, *Cx43* levels in the aldosterone-treated mice were only higher than the levels of the old mice. Cells were also counted, and we found that there was loss of cells between young adult and old animals, as expected with age. Fewer cells were also counted in the aldosterone-treated mice compared to the young adult animals; and we observed slightly more cells than the number found in untreated old animals.

Figures 19-22 show images of different regions of the cochleae for these three different subject groups.

3.4 Kir4.1 Expression Patterns Following Aldosterone Treatments Mimic That of Cx30 and Cx43

Cochlear samples from the same mice used in the aldosterone study were also stained to measure the protein expression of Kir4.1 receptors. Kir4.1 has been linked to gap junction proteins, such as connexins, in regulating the concentration of K^+. [69, 70] Downregulation of Kir4.1 expression between young adult and old animals was seen in all regions of the cochlea; moreover, the downregulation was statistically significant for the organ of Corti. Aldosterone-treated mice exhibited Kir4.1 levels comparable to those of young adult animals in all cochlear regions investigated, indicating a therapeutic effect. Cell loss associated with aging was seen between young adult and old mice. Young mice also exhibited higher cell numbers than that of the aldosterone-treated mice. Old comparison mice and aldosterone-treated old mice had similar cell counts on average (Figures 24-28). Cells were counted utilizing DAPI which labelled DNA within the nuclei of the cells.

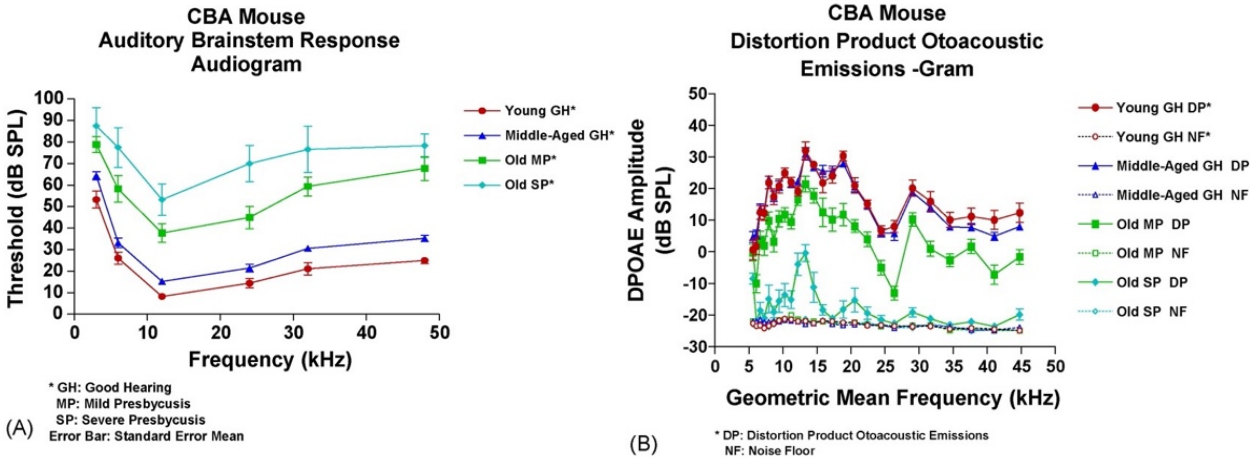

Figure 4. *A comparison of ABR thresholds and DPOAE amplitudes between different age groups.* A) Auditory brainstem responses (ABRs) for the four CBA mouse groups: young adult age group with good hearing, middle age group with good hearing, old age group with mild/moderate hearing loss, and old age group with severe hearing loss. (B) Distortion product otoacoustic emission (DPOAE) amplitudes for the same four groups of mice as in (A). From Tadros et al. (2007)

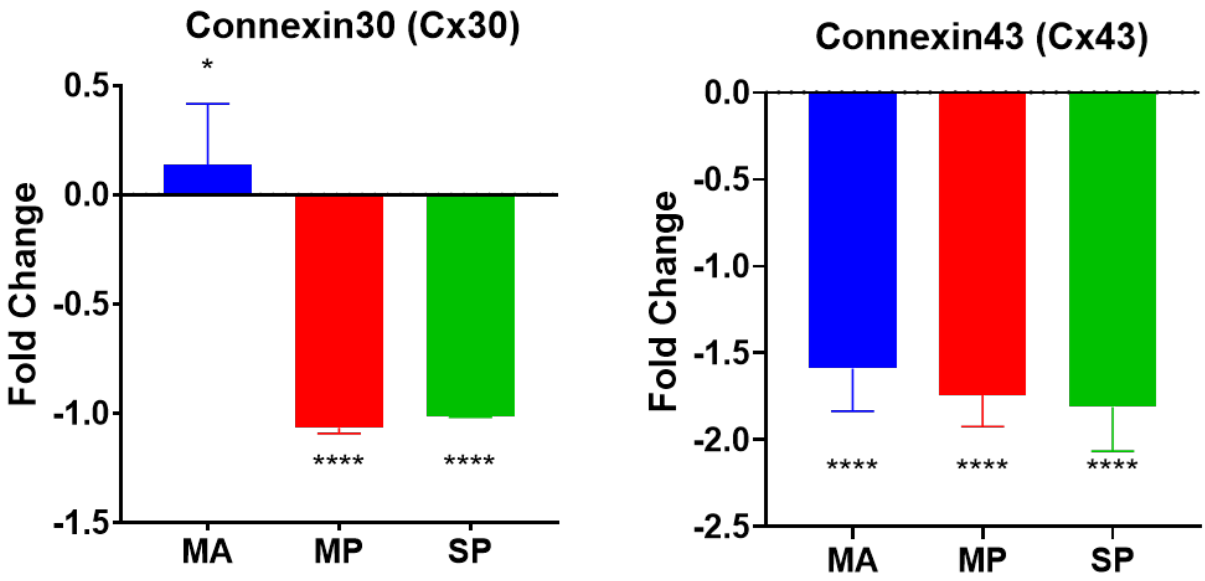

Figure 5. *Cx30 and Cx43 gene expression decreases with age.* Fold changes of (A) Cx30 and (B) Cx43 gene expression displayed significant downregulation in the GeneChip data collected from the cochlea of mild/moderate presbycusis, and severe presbycusis groups compared to the young adult control group. *p<.05, **p<.01, ***p<.001, ****p<.0001.

Table 1. ANOVA Results of Fold Change Values

Gene Name	**Average Fold Change**			**ANOVA**
	Middle Age	Mild Presbycusis	Severe Presbycusis	
Cx30	0.1370	-1.066	-1.014	**P=<0.0001,** F=17.34, df = 3,32
Cx43	-1.506	-1.743	-1.811	**P=<0.0001,** F= 34.65, df = 3,30

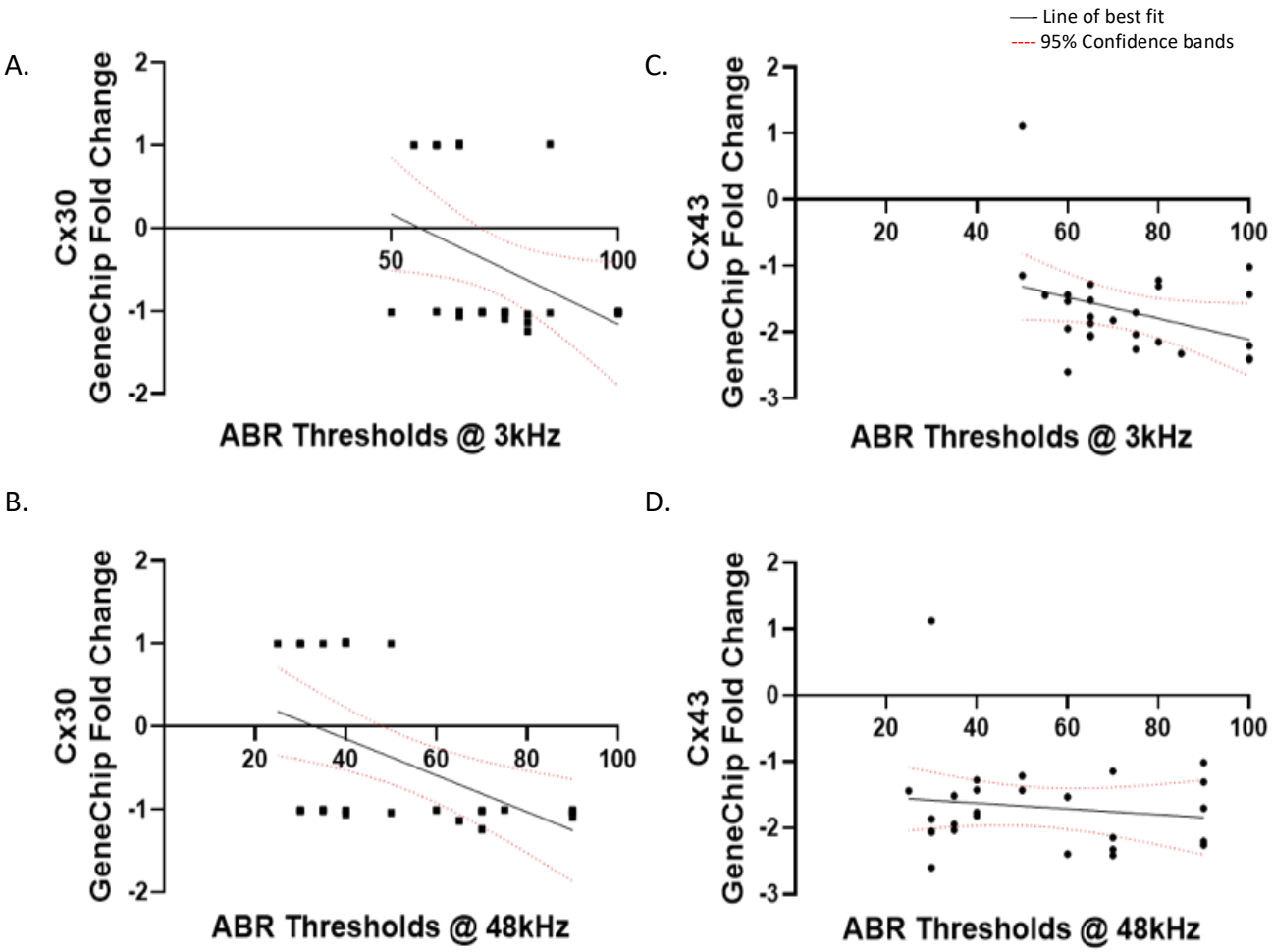

Figure 6. *Correlations found between ABR thresholds and fold changes.* ABR thresholds correlate with fold change gene expression changes for Cx30. (A-B) are examples of the significant correlations between ABR thresholds and Cx30 gene expression changes ($p<0.05$, 0.01, respectively). (C-D) shows correlations between Cx43 gene expression changes and ABR test results. The solid line in the graphs indicate the line of best fit and the dotted lines represent the 95% confidence intervals.

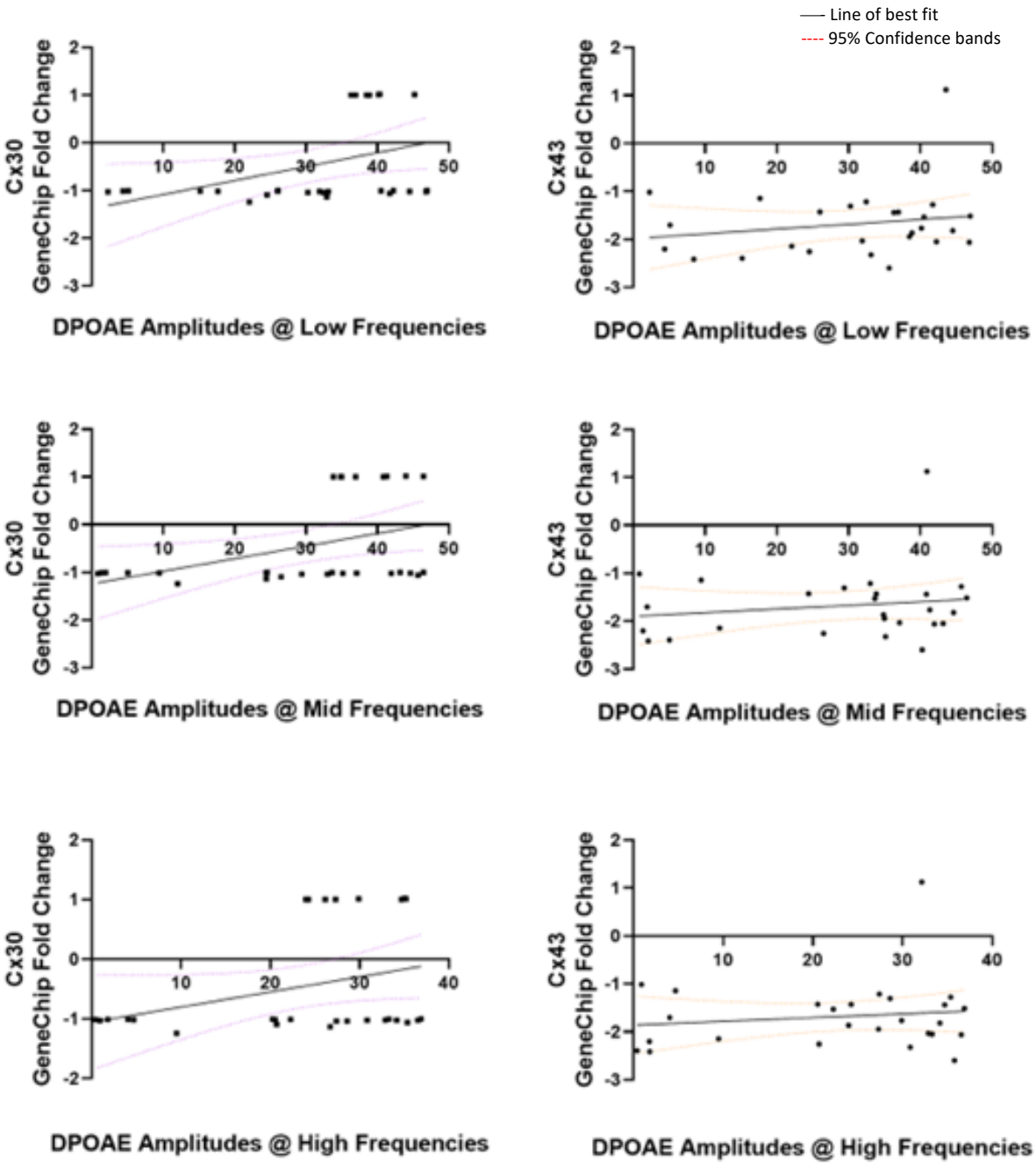

Figure 7. *DPOAE amplitude correlated with fold changes.* DPOAE amplitudes at low frequencies and mid frequencies showed significant correlations for Cx30 (Left column), but no significant correlations were found at high frequencies. There were no significant correlations seen between Cx43 fold changes and DPOAE amplitudes (Right column).

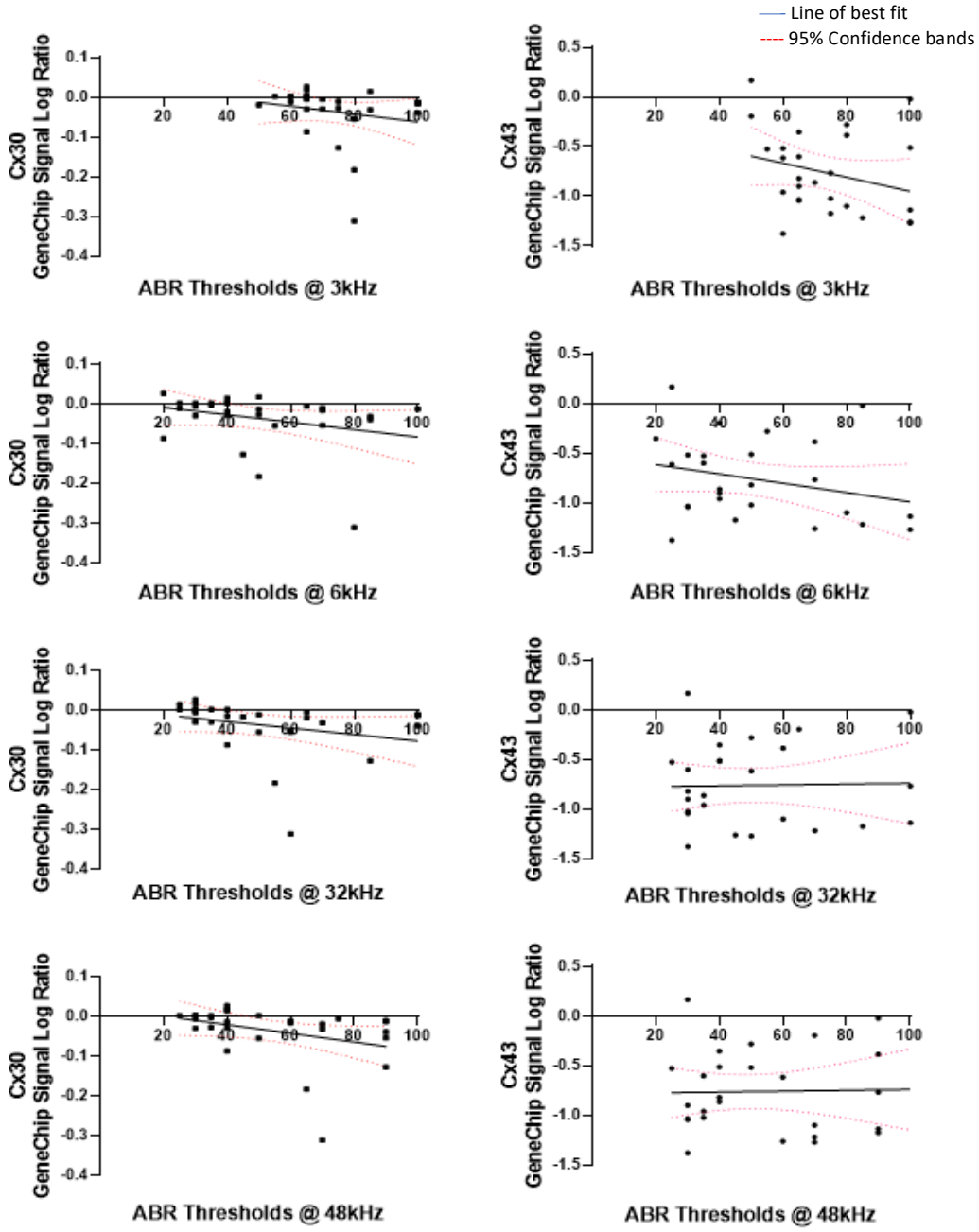

Figure 8. *ABR thresholds showed a trend of correlating with SLR.* ABR thresholds correlation with SLR gene expression of both Cx30 (left column) and Cx43 (right column) showed slight correlations at lower frequencies. At higher frequencies, only the SLR gene expression of Cx30 showed correlation. The solid line in the graphs indicate the line of best fit and the dotted lines represent the 95% confidence intervals.

Table 2. Correlations Between Gene Expression and Audiological Measurements

	Fold Change Correlation	
	Cx30	**Cx43**
ABR 3kHz	***P=0.0371**, r^2=0.1567, F=4.830	P=0.0756, r^2=0.1257, F=3.449
ABR 6kHz	***P=0.0229**, r^2=0.1836, F=5.847	P=0.1168, r^2=0.0993, F=2.647
ABR 12kHz	****P=0.0090**, r^2=0.2343, F=7.958	P=0.3634, r^2=0.0345, F=0.8585
ABR 24kHz	****P=0.0083**, r^2=0.2390, F=8.166	P=0.3862, r^2=0.0314, F=0.7790
ABR 32kHz	****P=0.0048**, r^2=0.2677, F=9.505	P=0.6600, r^2=0.0081, F=0.1984
ABR 48kHz	****P=0.0046**, r^2=0.2700, F=9.616	P=0.4691, r^2=0.0191, F= 0.4691
DPOAE Low Freq.	***P=0.0360**, r^2=0.1583, F=4.891	P=0.3529, r^2=0.0360, F=0.8975
DPOAE Mid Freq.	***P=0.0285**, r^2=0.1715, F=5.382	P=0.4177, r^2=0.0275, F=0.6800
DPOAE High Freq.	P=0.0971, r^2=0.1023, F=2.962	P=0.4920, r^2=0.0198, F=0.4870

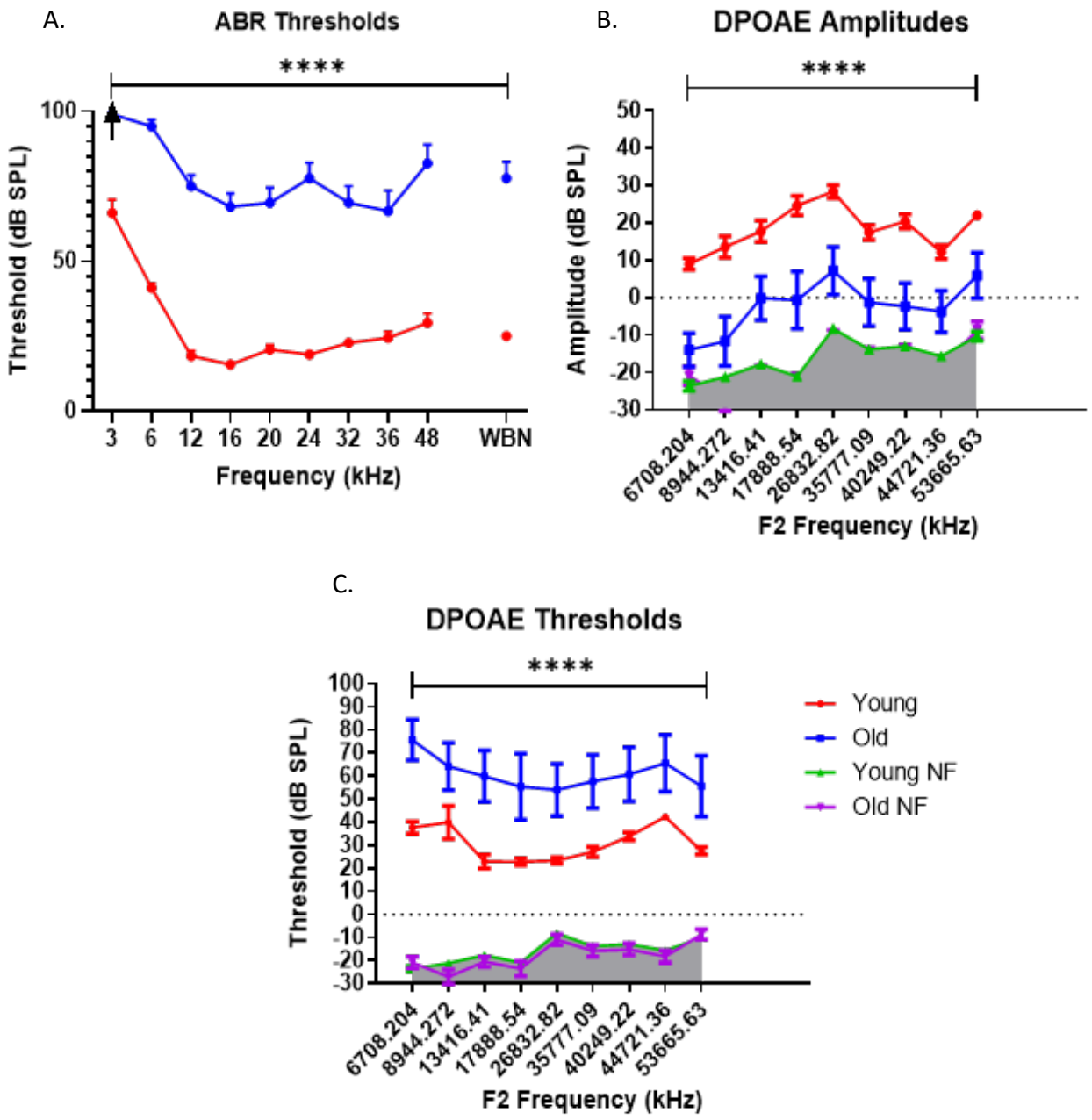

Figure 9. *ARHL was seen between young and old subject groups*. Young adult and old hearing comparisons for (A) ABR thresholds, (B) DPOAE amplitudes, and (C) DPOAE thresholds for frequencies ranging from 3-53.6kHz. All hearing tests demonstrated a significant increase in ABR and DPOAE thresholds for the old animals compared to the young adults. The DPOAE amplitudes are also significantly decreased; thus, validating that age-related hearing loss is occurring. *p<.05, **p<.01, ***p<.001, ****p<.0001

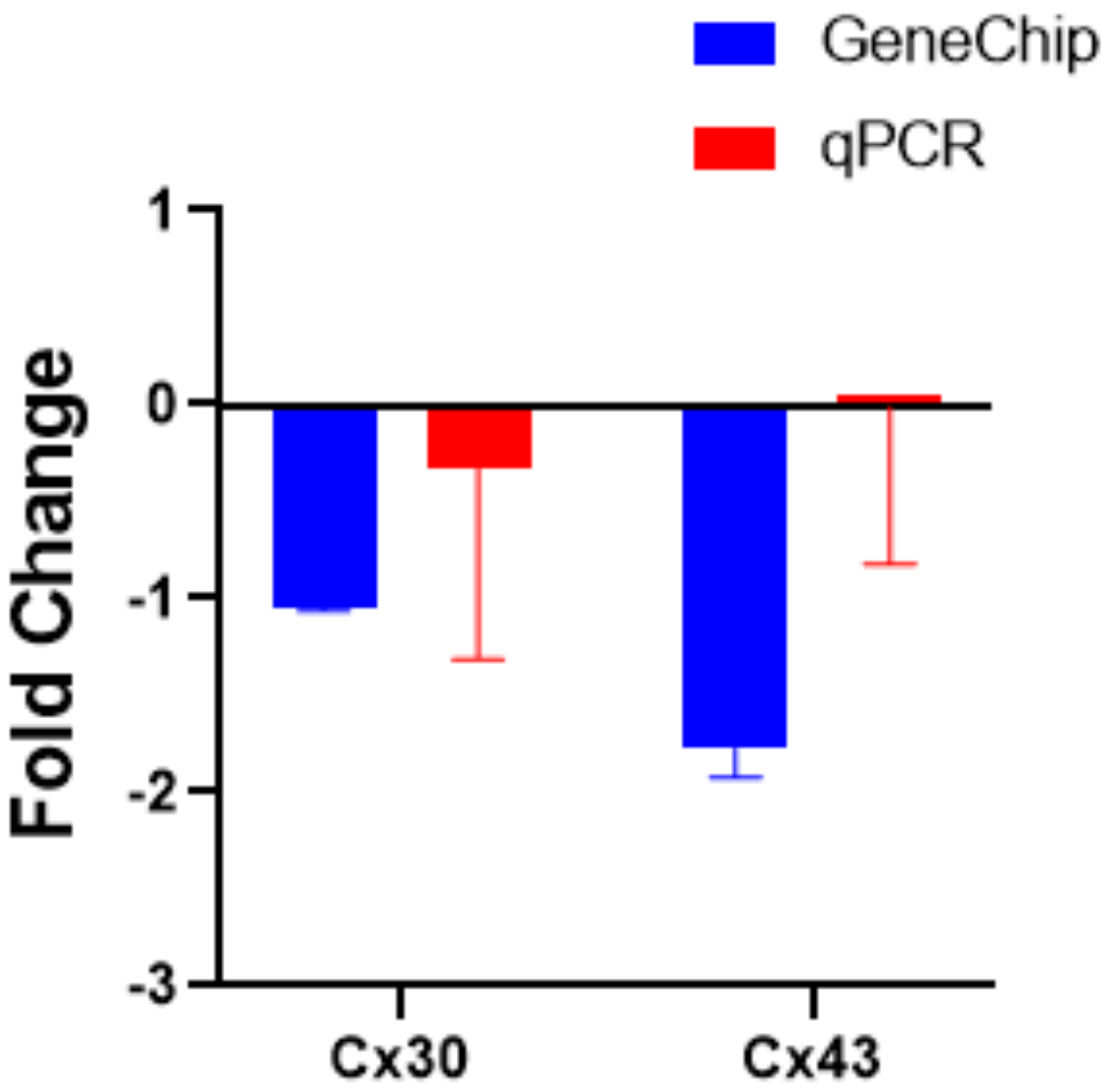

Figure 10. *Gene expression fold changes from RT-qPCR and GeneChip displayed downregulation for both Cx genes.* Fold changes obtained from real-time PCR and GeneChip for Cx30 and Cx43 in the cochlea showed downregulation with age and hearing loss.

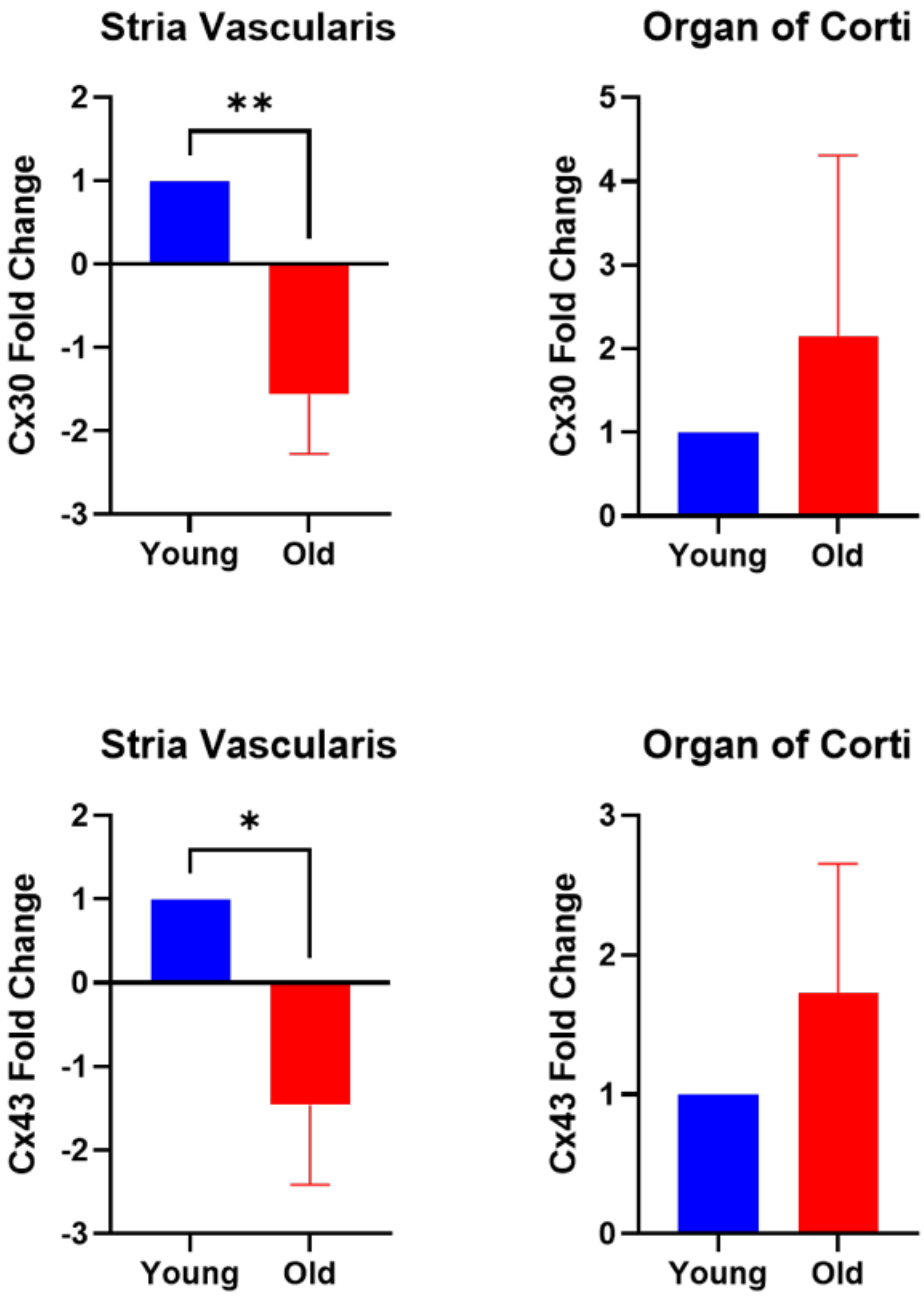

Figure 11. *RT-qPCR results show differences in Cx30 and Cx43 gene expression with age.* Results from qPCR triplicate experiments showed a significant fold change difference in Cx30 and Cx43 between young and old animals in the stria vascularis (left column). There were no significant changes found with age in the organ of Corti for both genes (right column). *p<.05, **p<.01

Table 3. t-test Results from Animal Tissue RT-qPCR

Gene Name	**t-test**	
	SV	OC
Cx30	****P=0.0050**, t=3.578, df=10	P=0.6238, t=0.5305, df=4
Cx43	***P=0.0269**, t=2.592, df=10	P=0.4544, t= 0.7862, df =8

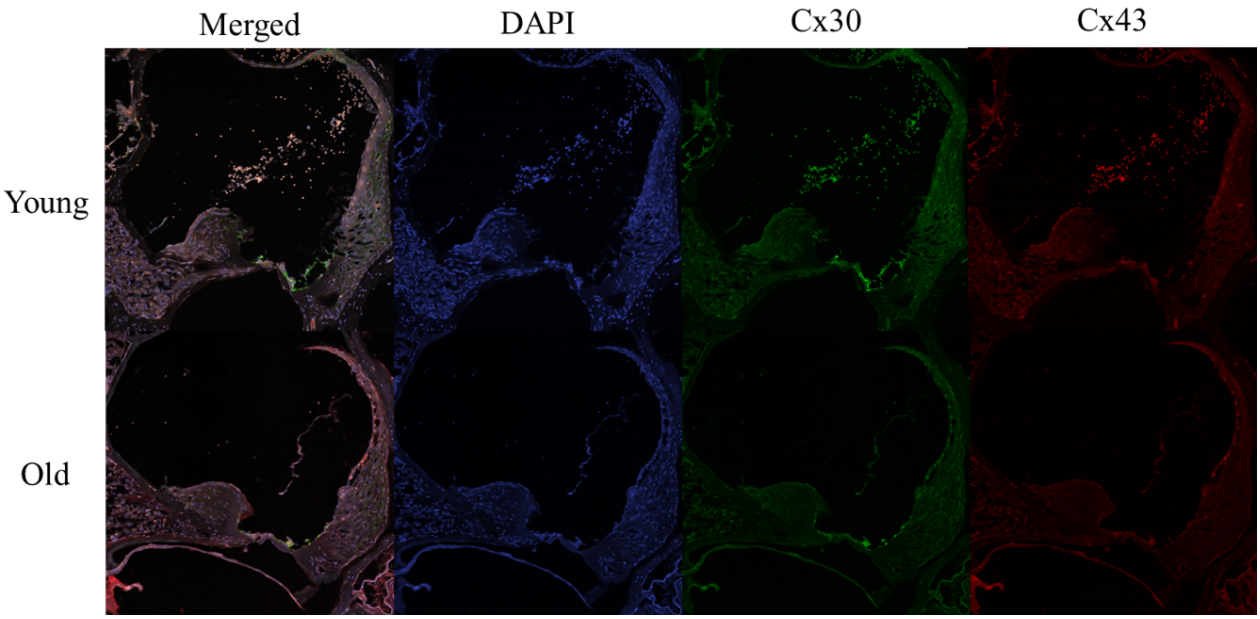

Figure 12. *Cx30 and Cx43 protein expression decreased between young and old mice*. Full view of the basal turn of the cochlea shows the decrease of Cx30 (green) and Cx43 (red) immunofluorescence with age.

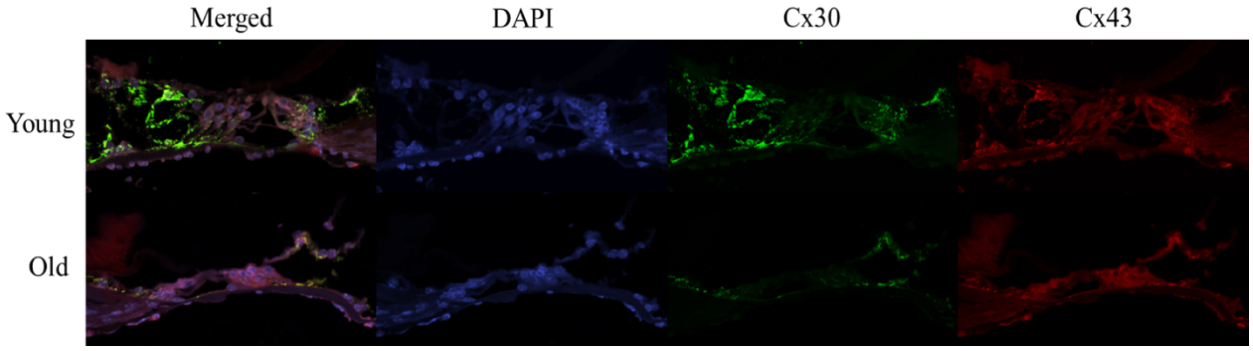

Figure 13. *Downregulation of Cx30 (green) and Cx43 (red) in the OC in the apical region of the mouse cochlea.*

Table 4. One-Way ANOVA Aging Results

Gene Name	**ANOVA**		
	SV	OC	SGN
Cx30	*Apex*: ***P=0.0387** t=2.917 df=12	*Apex*: P=0.3932 t=1.621 df=12	*Apex*: P=>0.9999 t=0.5543 df = 11
	Mid: P=0.2035 t=2.007 df=12	*Mid:* ***P=0.0069** t=3.852 df=12	*Mid:* P=>0.9999 t=0.6665 df=11
	Basal: P=0.0802 t=2.524 df=12	*Basal:* ***P=0.0227**, t=3.204, df=12	*Basal:* P=0.5271 t=1.447 df=11
Cx43	*Apex*: P=0.7648 t=1.196 df=12	*Apex*: P=0.9954 t=1.011 df=12	*Apex*: P=>0.9999 t=0.1978 df=11
	Mid P=0.8035 t=1.162 df=12	*Mid:* P=>0.9999 t=0.4525 df=12	*Mid:* P=>0.9999 t=0.2394 df=11
	Basal: P=0.3808 t=1.640 df=12	*Basal:* P=0.7508 t=1.208 df=12	*Basal:* P=0.8715 t=1.110 df=11

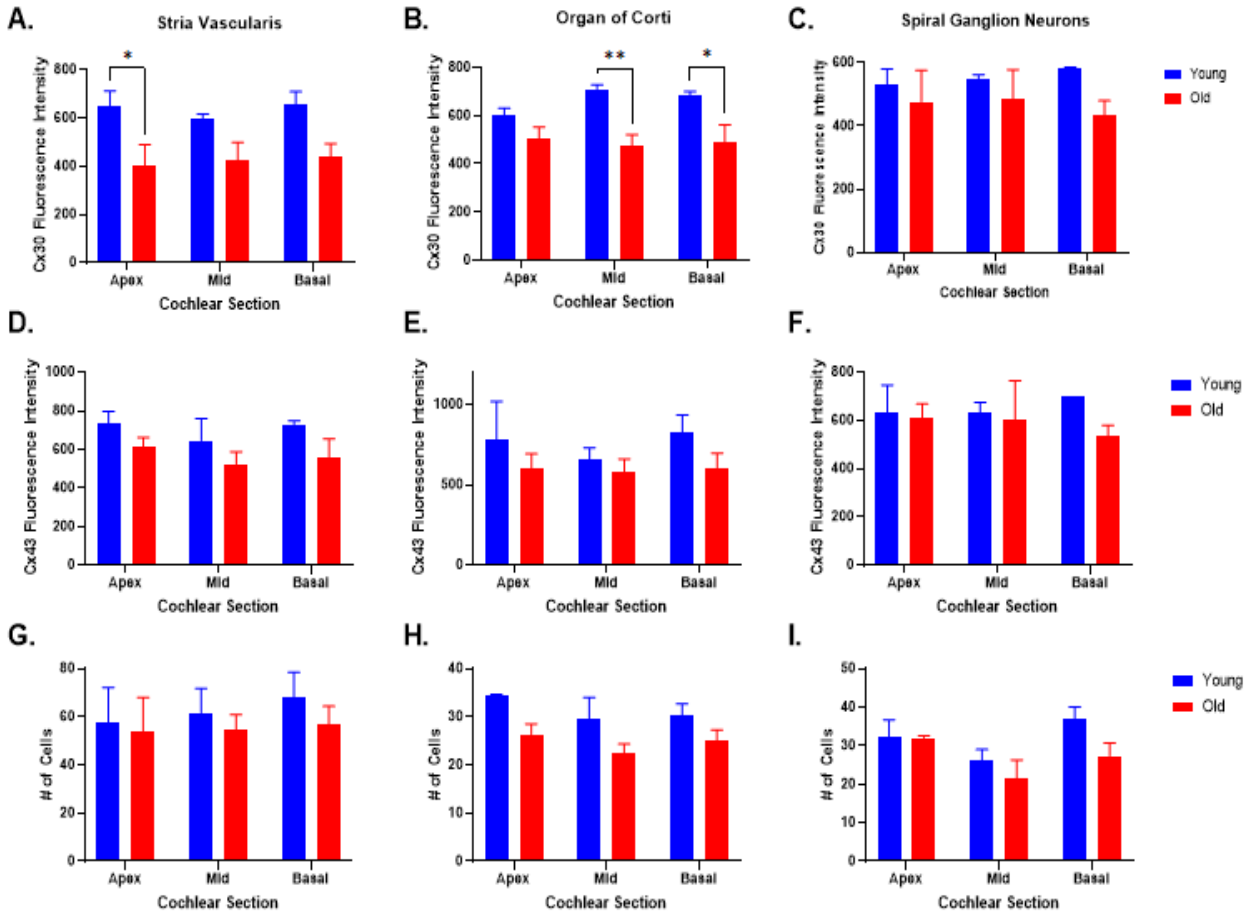

Figure 14. *Cx30 and Cx43 protein expression decreased in various areas of the cochlea.* Decreases in Cx30 and Cx43 protein expression was observed between young adult and old animals in all regions of the cochlea. Statistically significant downregulation was seen in the SV in the apex, and in the OC in the middle and basal turns. Cell counts were lower in old animals, consistent with the effects of aging.

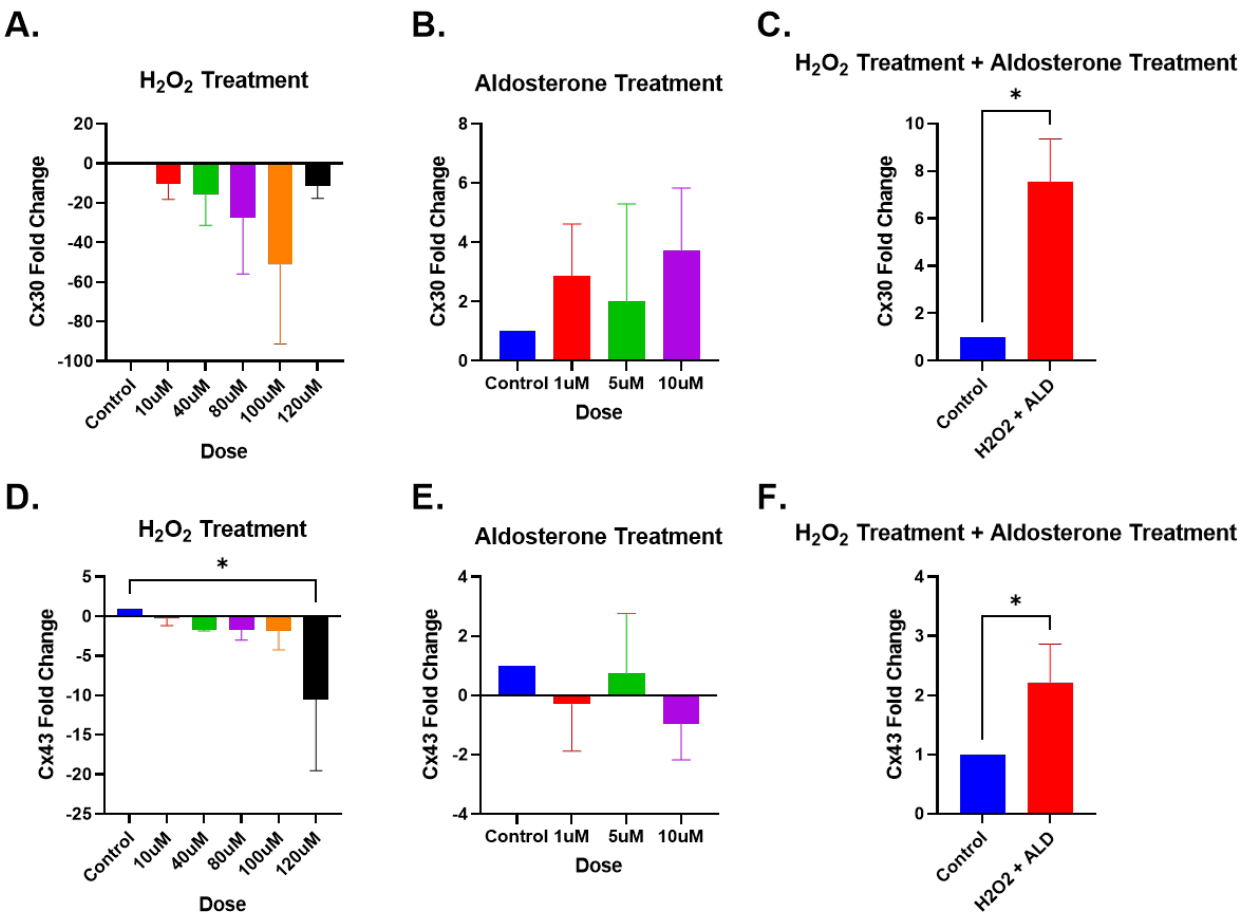

Figure 15. *H_2O_2 and aldosterone treatment changes Cx gene expression*. Gene expression of *Cx30* and *Cx43* decreased in the SV-k1 cell line following 24-hr treatment with (A and D) H_2O_2 at multiple doses; but increased for *Cx30* after being treated with (B) aldosterone, but not much change for *Cx43* (E). (C) shows a significant upregulation of Cx30 gene expression following the combination treatment of H_2O_2 and aldosterone. (F) also revealed an upregulation of Cx43 after the combination treatment. *p<.05

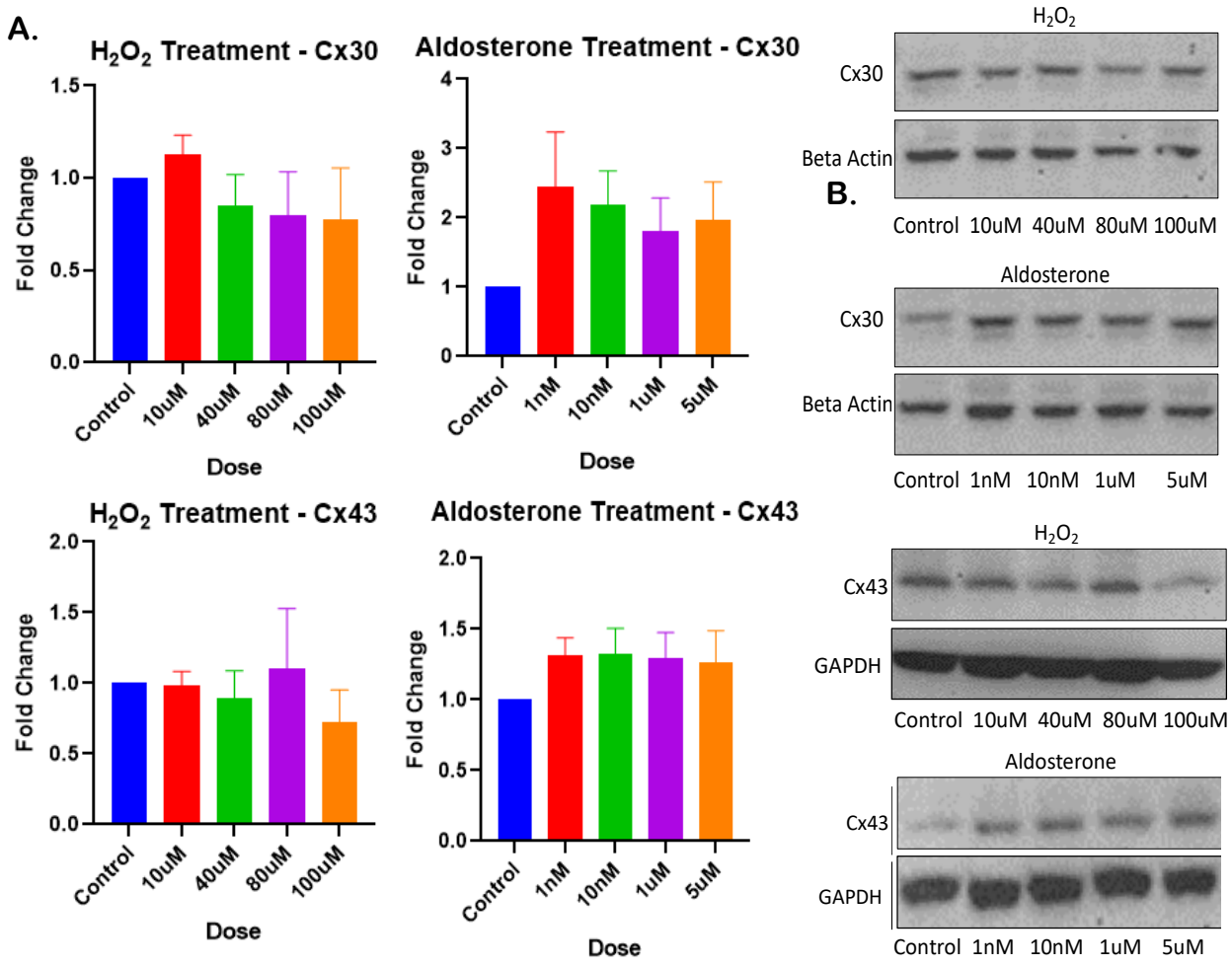

Figure 16. *Cx protein expression is modulated by H_2O_2 and aldosterone.* (A) Densitometry and (B) gel images show that the protein expression of Cx30 and Cx43 decreased following 24hour H_2O_2 treatment at all doses, except at 10uM for Cx30 and 80uM for Cx43. Aldosterone caused the expression of both Cx proteins to increase for all doses.

Table 5. t-Test Results for Cell Treatments

Treatment		
	Cx30	Cx43
H_2O_2 120µM	P=>0.9999 t=0.4158 df=59	***P=0.035** t=2.949 df=24
H_2O_2 + Aldosterone	***P=0.0221** t=3.632 df=4	***P=0.0368** t=3.085 df=4

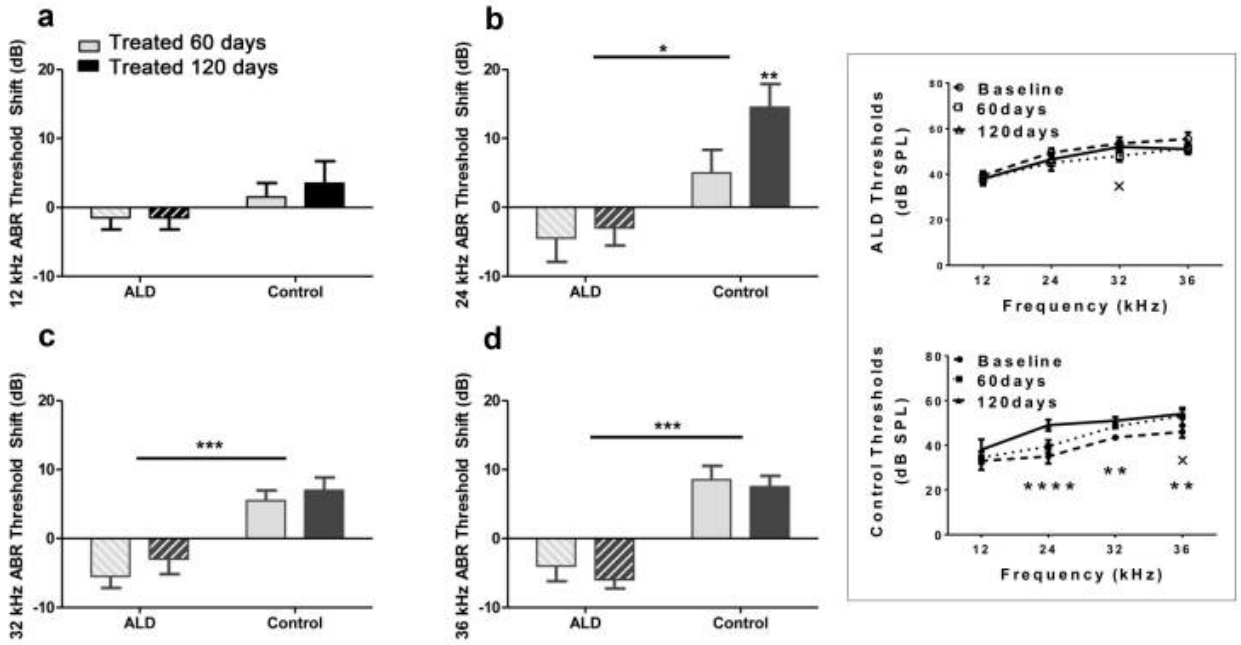

Figure 17. *ABR threshold shifts at (A) 12, (B) 24, (C) 32, and (D) 36kHz showed improved hearing sensitivity, with a larger protective effect seen at higher frequencies.* Negative shifts indicate improved hearing. (Right column) ABR thresholds for aldosterone-treated mice had very little change over the 4 months while control mice showed age-related hearing loss elevations. +$p<0.05$ for 60 days; *$p<0.05$ for 120 days; **$p<0.01$ for 120 days, ****$p<0.0001$ for 120 days. This figure is taken from Frisina et al. (2016) with permission.

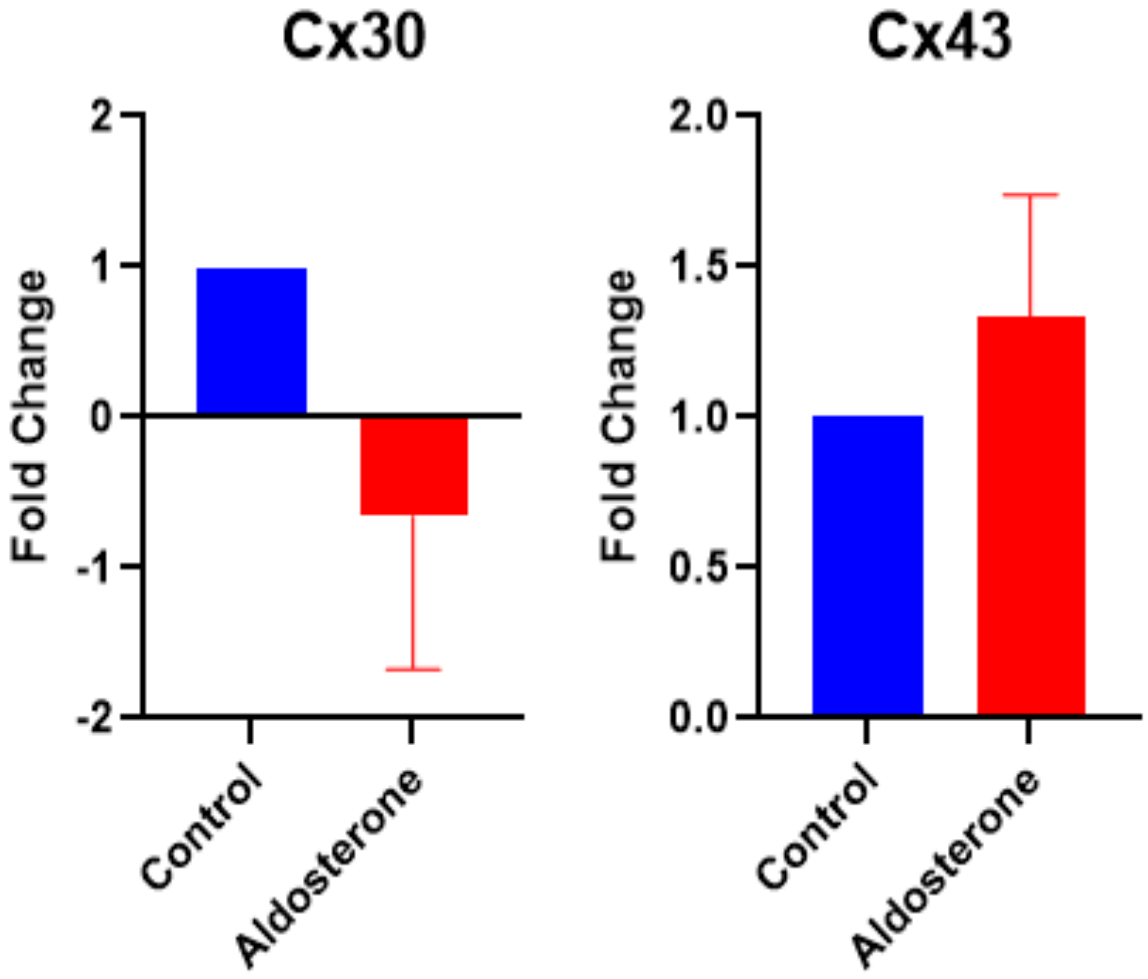

Figure 18. *In vivo aldosterone treatment does not cause significant changes in Cx43 and Cx30 gene expression.* Triplicate qPCR experiments show some trends but resulted in no significant fold change difference in Cx30 and Cx43 between control and aldosterone-treated animals.

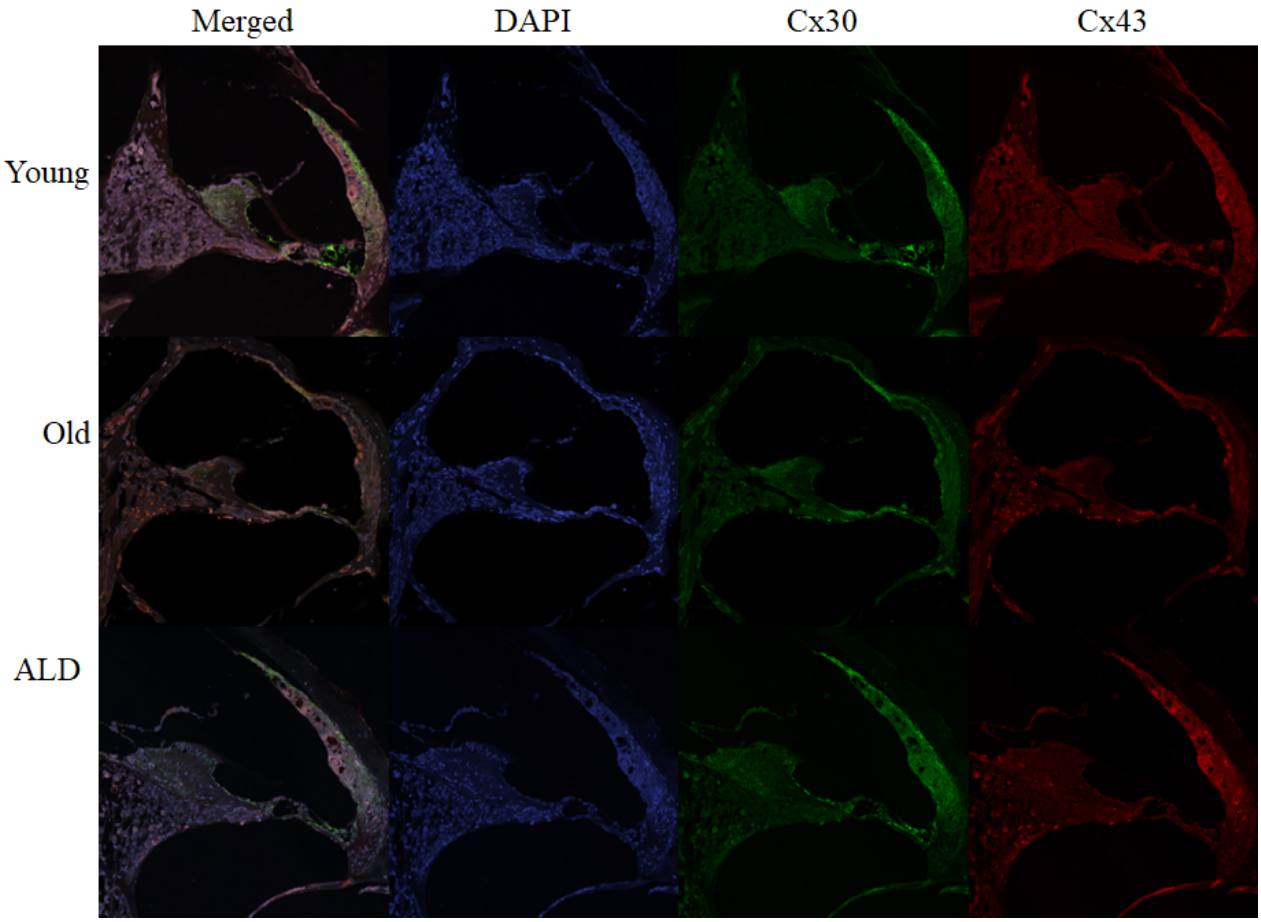

Figure 19. *Cx protein expression increased in the mouse cochlea following long-term aldosterone treatment.* The expression of Cx30 (green) and Cx43 (red) visibly decreased between young adult and old animals. Aldosterone treatment maintained the expression of Cx43 comparable to that of young adult animals, but significantly increased the expression of Cx30 compared to old animals in the SV, OC, and SGN (third row).

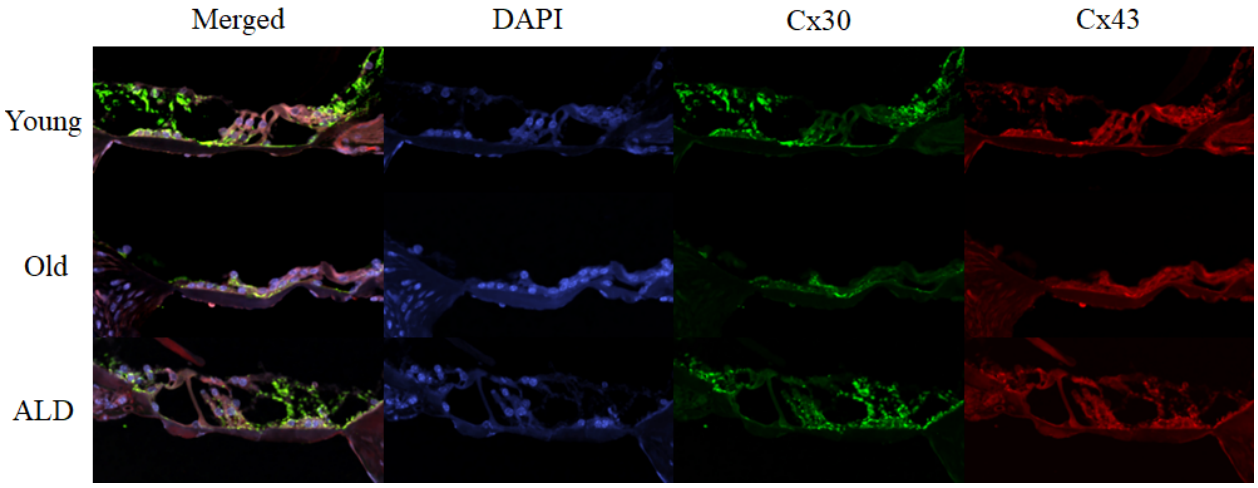

Figure 20. *Aldosterone upregulated Cx protein expression in the OC.* In the OC, Cx30 (green) was significantly upregulated in the aldosterone-treated mice compared to old comparison mice. Cx43 (red) protein expression was also higher in the mice treated with aldosterone compared to old mice of the same age. This figure shows the OC in the middle turn of the cochlea. DAPI, blue, labels cell nuclei.

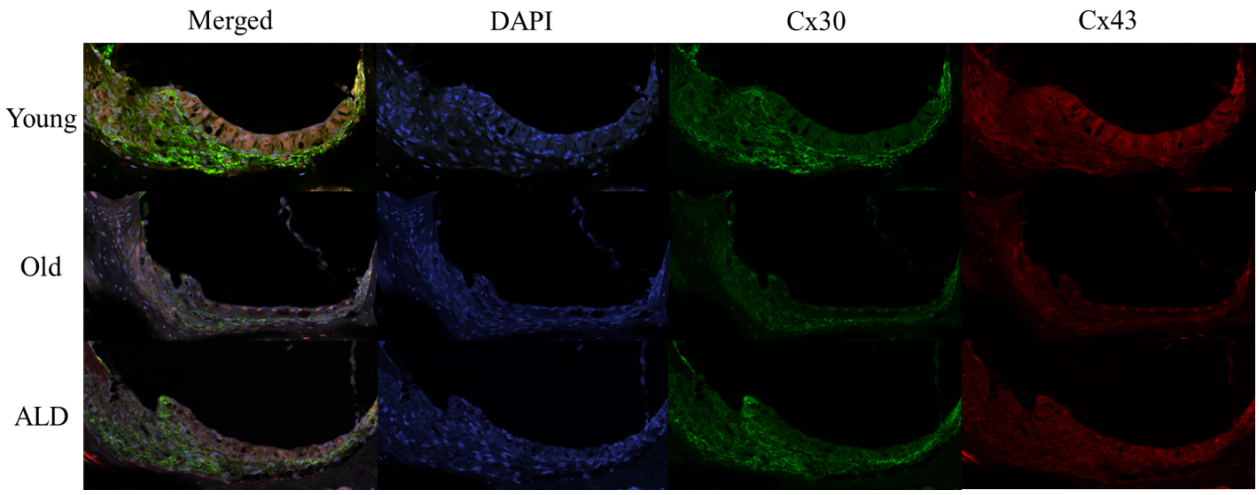

Figure 21. *Higher Cx30 and Cx43 expression is observed in aldosterone-treated mice compared to old mice.* In the SV, expression of both, Cx30 and Cx43, was higher in aldosterone-treated animals compared to old animals. Cx30 protein expression was statistically significantly higher in the aldosterone mice when compared to the old mice.

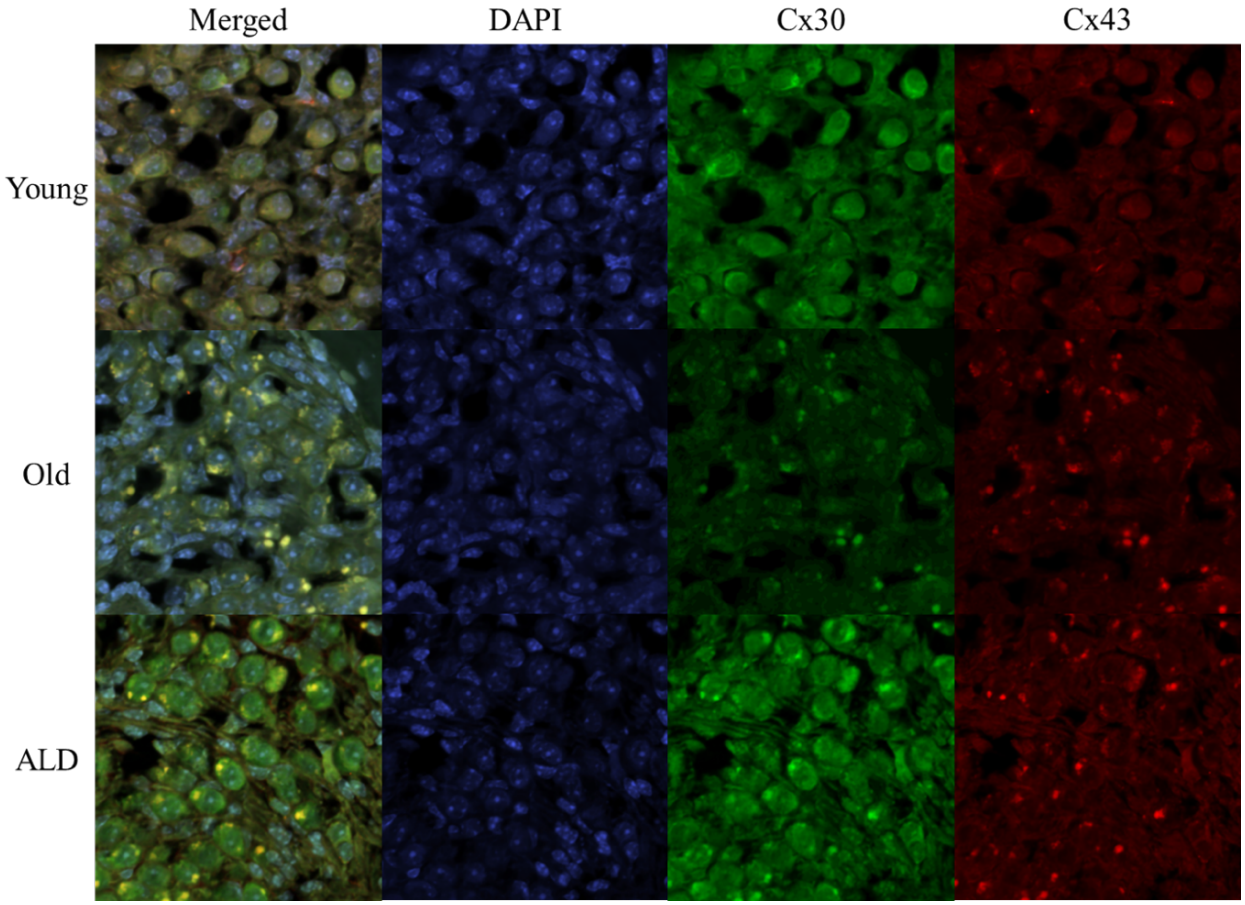

Figure 22. *Cx expression in SGNs is higher in aldosterone-treated animals.* Cx protein expression was also higher in aldosterone-treated mice compared to young adults in the SGN in all three turns of the cochlea. The expression of Cx30 was also statistically significantly higher in all three turns compared to old animals.

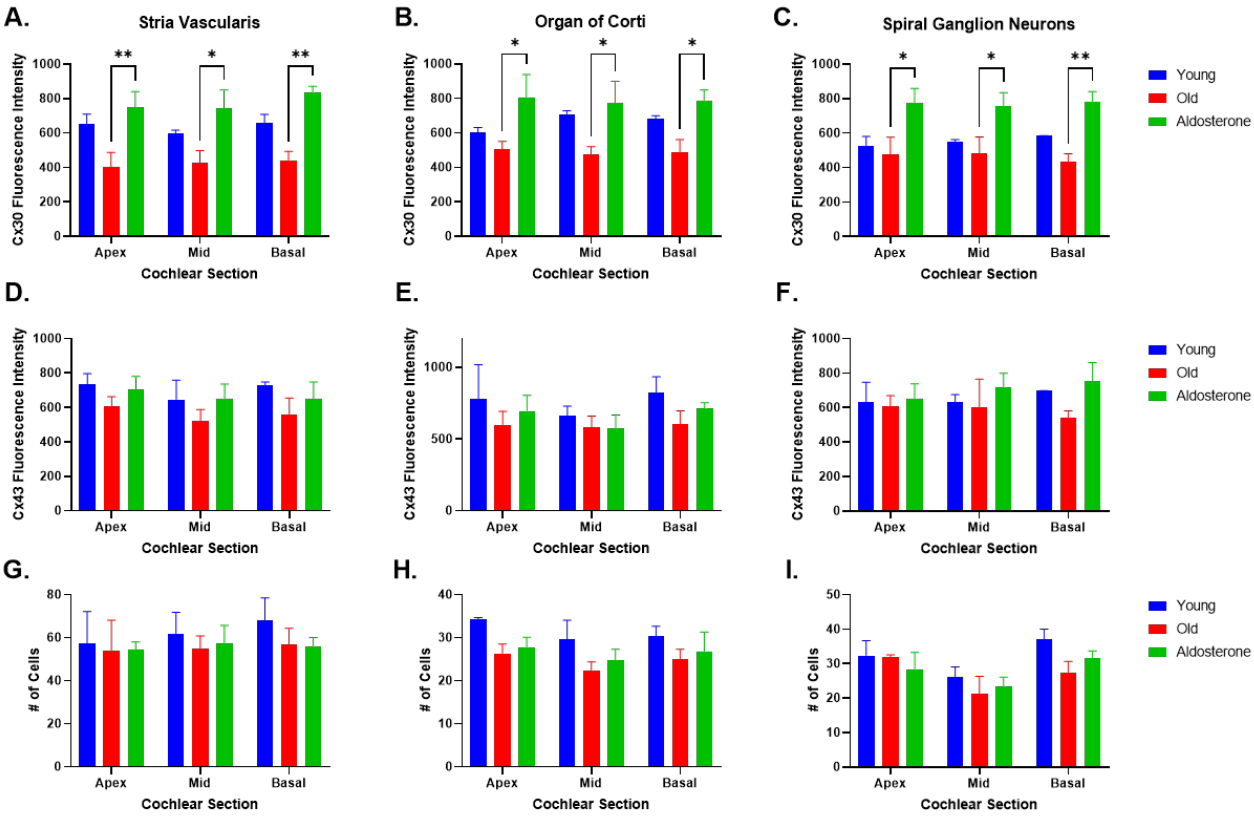

Figure 23. *Quantitative immunohistochemistry results showed aldosterone protected Cx30 and Cx43 protein expression levels.* Cx30 and Cx43 protein expression were seen to decrease between young adult and old animals; yet a significant increase of Cx30 was seen in aldosterone-treated animals compared to old animals of the same age in the (A) SV, (B) OC, and (C) SGN. Moreover, Cx30 expression in aldosterone-treated animals was even higher than young adult animals. Aldosterone-treated animals also showed higher Cx43 protein levels compared to old mice of the same age (D-F). Normal, age-related cell loss was observed between young adult and old mice. Although a trend for aldosterone protecting cells in the old cochlea is apparent in G-I, the number of cells in aldosterone-treated old mice were about the same as that found in the old comparison mice (G-I). *$p<0.05$, **$p<0.01$

Table 6. Bonferroni Results from Aldosterone Treatment for Protein Expression Changes

Protein Name	**ANOVA**		
	SV	OC	SGN
Cx30	*Apex***: **P=0.0064,** t=3.582, df=18	*Apex***: *P=0.0314,** t=2.857**,** df=18	*Apex***: *P=0.0223,** t=3.028, df = 17
	Mid: ***P=0.0137,** t=3.238**,** df=18	*Mid:* ***P=0.0310,** t=2.864**,** df=18	*Mid:* ***P=0.0364,** t=2.806**,** df=17
	Basal: ****P=0.0024,** t=4.017**,** df=18	*Basal:* ***P=0.0354,** t=2.802**,** df=18	*Basal:* ****P=0.0075,** t=3.540**,** df=17
Cx43	*Apex***:** P=>0.9999, t=0.8679, df=18	*Apex***:** P=>0.9999, t=0.5813, df=18	*Apex***:** P=>0.9999**,** t=0.3242**,** df=17
	Mid: P=0.8647, t=1.094, df=18	*Mid:* P=>0.9999, t=0.0148, df=18	*Mid:* P=>0.9999, t=0.8566, df=17
	Basal: P=>0.9999, t=0.8167, df=18	*Basal:* P=>0.9999, t=0.6591, df=18	*Basal:* P=0.8715, t=1.658, df=17

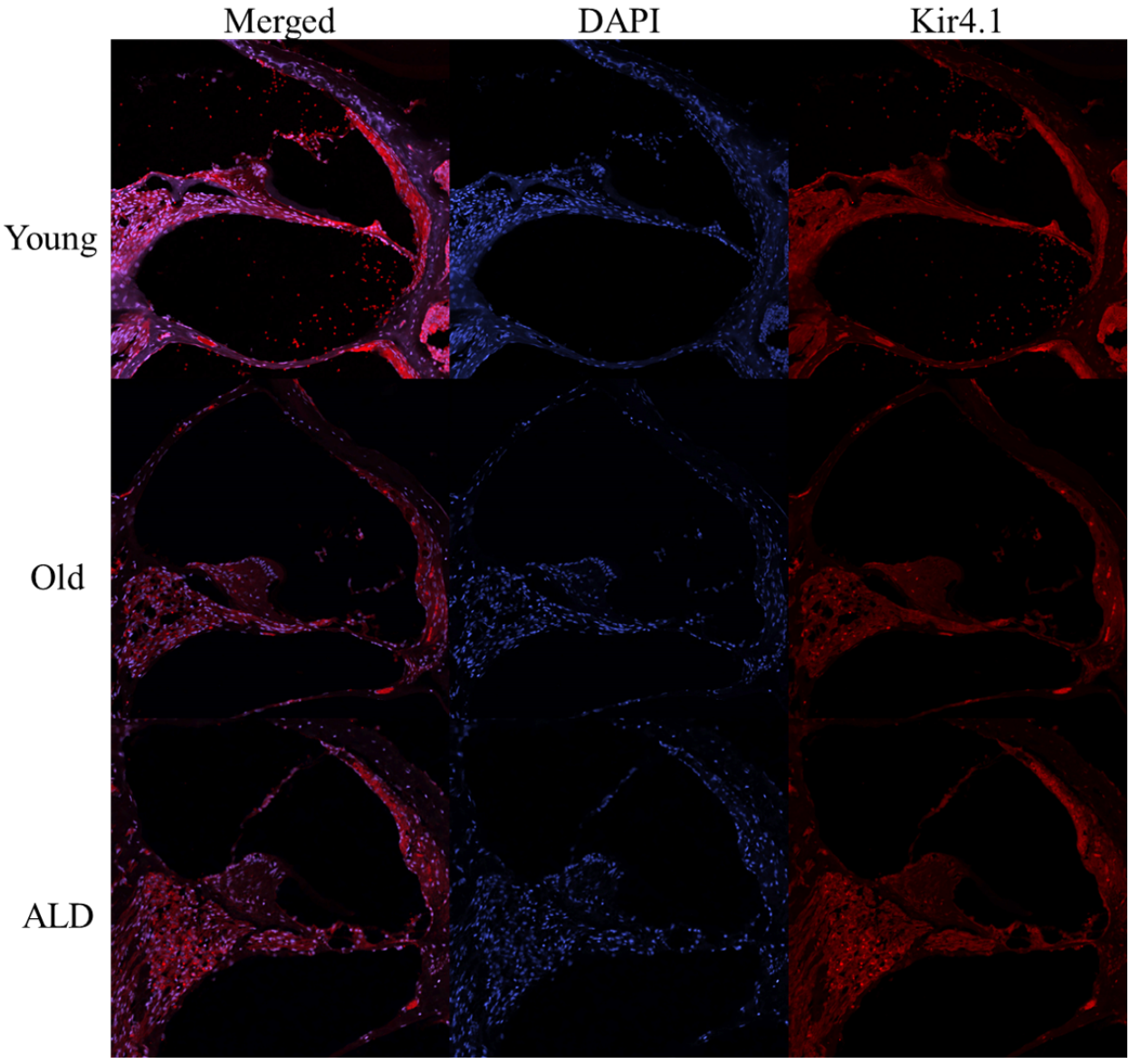

Figure 24. *Expression of Kir4.1 changes with age and aldosterone treatment.* Kir4.1 protein expression was downregulated between young adult and old animals as seen here in the apex of the cochlea; however, aldosterone-treated old mice had Kir4.1 expression levels similar to young adult animals overall.

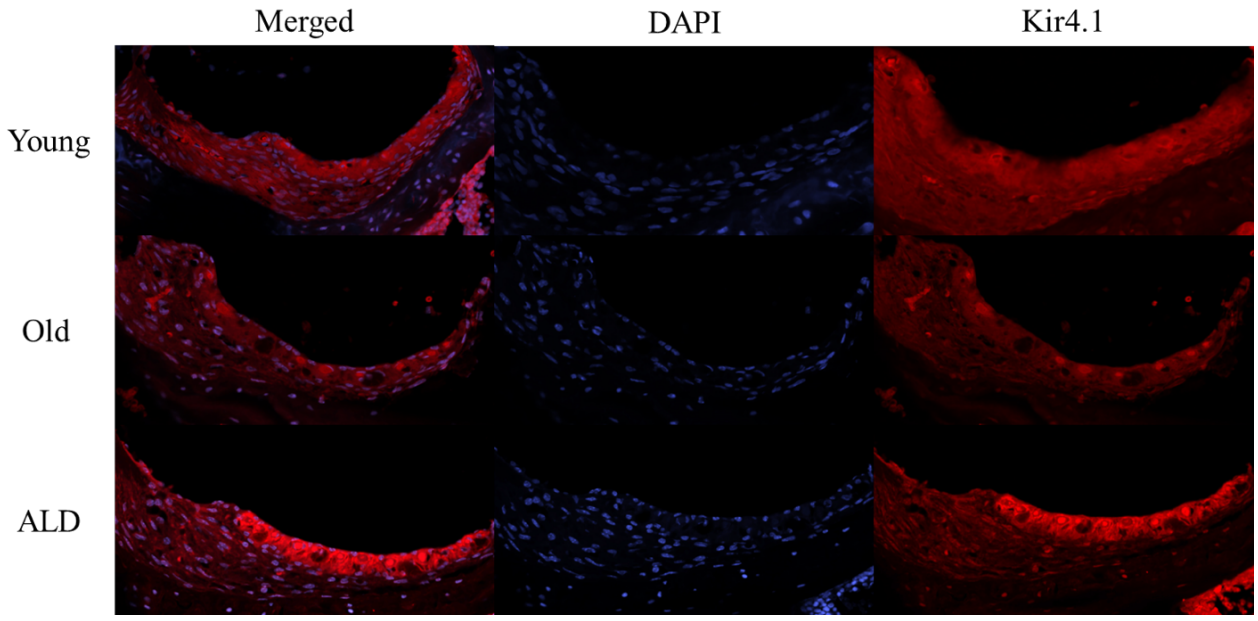

Figure 25. *Aldosterone upregulated Kir4.1 protein expression in the SV.* Similar to the OC, protein expression levels of Kir4.1 were enhanced in SV for the aldosterone-treated old mice, while old comparison mice displayed lower levels of Kir4.1 compared to the young adults and aldosterone-treated mice.

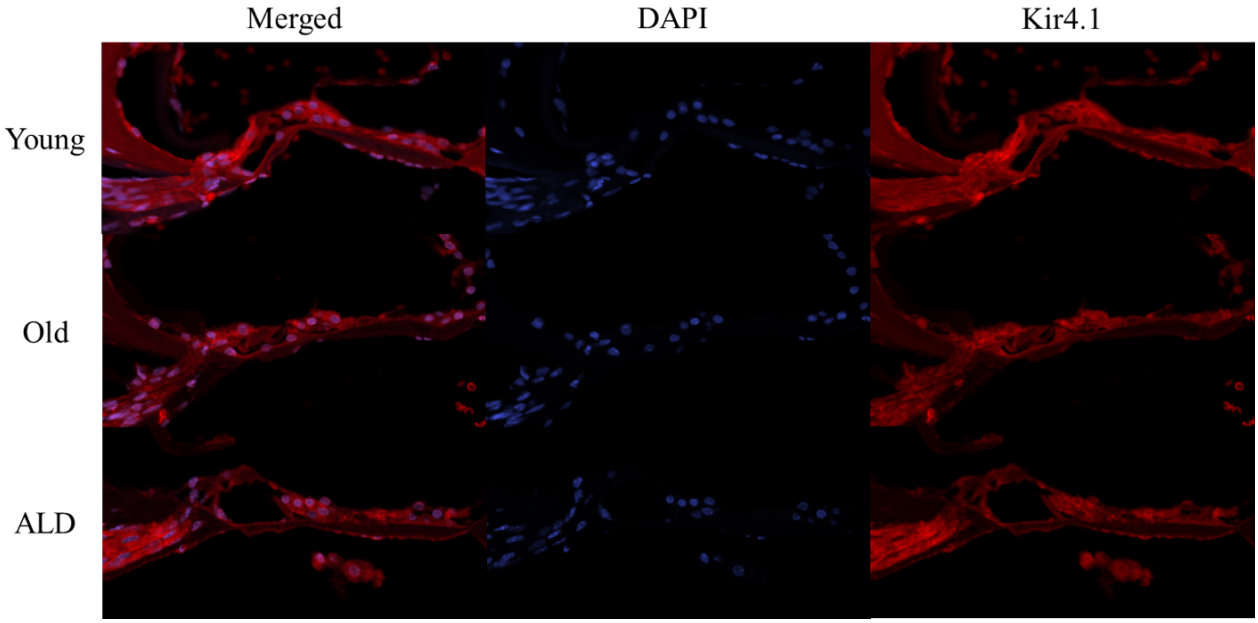

Figure 26. *Immunohistochemistry results in the OC shows differences in Kir4.1 with age and aldosterone treatment.* Significant downregulation of Kir4.1 in the OC was noted in old animals compared to young adult control animals, specifically in the apex and middle turns. Old mice treated with aldosterone exhibited levels higher than that of the old comparison mice. This indicates that aldosterone has protective effects in the OC.

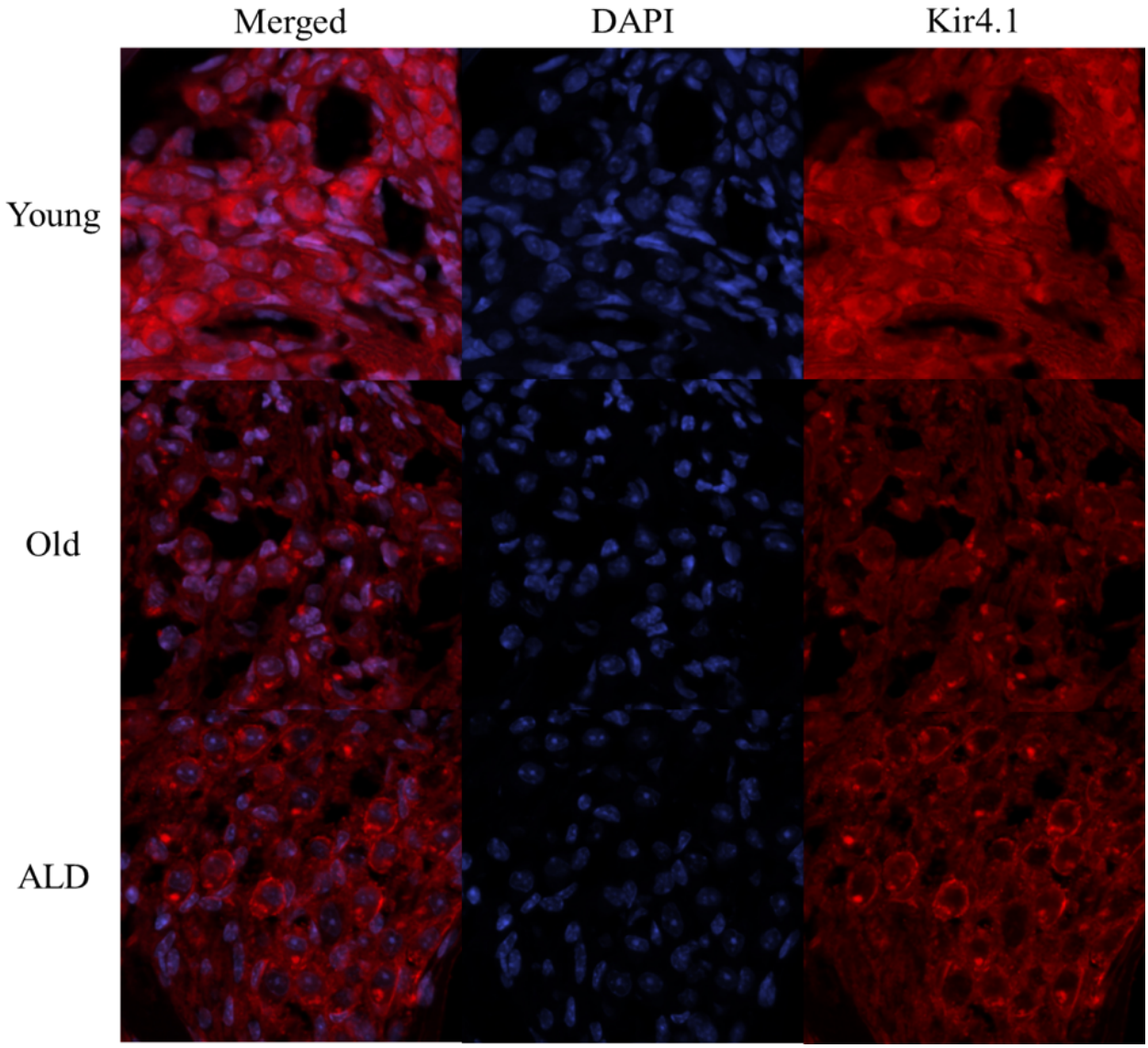

Figure 27. *Protective effects of aldosterone were observed in the SGNs.* Kir4.1 protein expression decreased in MD for the SGNs with age. However, animals treated with aldosterone exhibited levels that were higher than old comparison mice, showing that aldosterone can help rescue Kir4.1 receptor protein expression levels. DAPI stains cell nuclei.

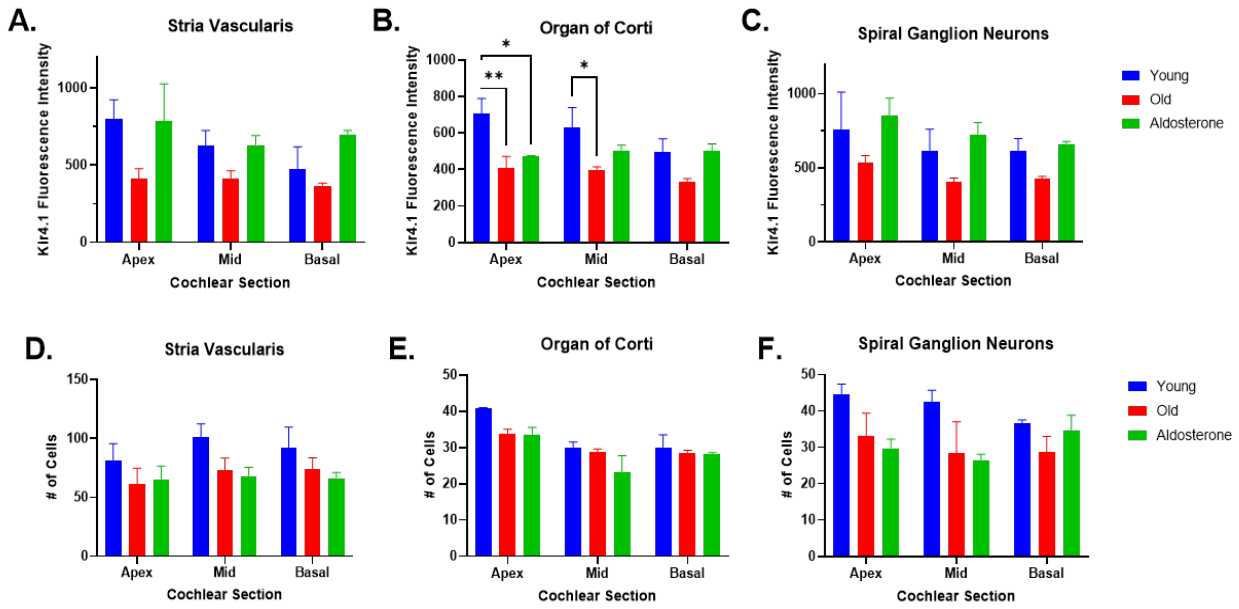

Figure 28. *Quantitative results indicate that aldosterone protects Kir4.1 protein expression in all regions of the cochlea.* Aldosterone-treated mice showed Kir4.1 receptor protein expression levels like those of young adult animals, while old comparison animals showed less expression compared to the other two groups. There was statistically significant downregulation between young and old mice in the organ of Corti (B). (D-F) Cell counts showed that both old and aldosterone-treated old mice tended to have lower numbers of cells compared to young adult animals. *p<.05, **p<.01

Table 7. Bonferroni Test of Kir4.1 Expression

	SV	**OC**	**SGN**
Young vs. Old	*Apex*: P=0.0820 t=2.402 df=18	*Apex***: **P=0.0074** t=3.515 df=18	*Apex***:** P=0.5531 t=1.380 df = 18
	Mid: P=0.5706 t=1.361 df=18	*Mid:* ***P=0.0348** t=2.810 df=18	*Mid:* P=0.6162 t=1.314 df=18
	Basal: P=>0.9999 t=0.7238 df=18	*Basal:* P=0.1774 t=2.015 df=18	*Basal:* P=7477 t=1.191 df=18
Young vs. Aldosterone	*Apex***:** P=>0.9999 t=0.056 df=18	*Apex***: *P=0.034** t=2.800 df=18	*Apex***:** P=>0.9999 t=0.580 df=18
	Mid: P=>0.9999 t=0.025 df=18	*Mid:* P=0.4453 t=1.510 df=18	*Mid:* P=>0.9999 t=0.671 df=18
	Basal: P=0.5597 t=1.373 df=18	*Basal:* P=>0.9999 t=0.081 df=18	*Basal:* P=>0.9999 t=0.257 df=18
Old vs. Aldosterone	*Apex***:** P=0.0920 t=2.345 df=18	*Apex***:** P=>0.9999 t=0.7146 df=18	*Apex***:** P=0.1968 t=1.961 df=18
	Mid: P=0.5472 t=1.387 df=18	*Mid:* P=0.6303 t=1.300 df=18	*Mid:* P=0.1878 t=1.985 df=18
	Basal: P=>0.1512 t=2.097 df=18	*Basal:* P=0.1514 t=1.300 df=18	*Basal:* P=0.4941 t=1.448 df=18

Chapter 4: Discussion

4.1 Changes in Cx30 and Cx43

While mutations in connexin gap junction proteins have been shown to be one of the main causes of congenital deafness, the possibility of these proteins having a role with presbycusis has not been investigated systematically, until now. Our hypothesis is that changes in connexin protein expression, affecting cochlear gap junction structure and functionality, contributes to the development of ARHL. The present study demonstrated age-related hearing impairment in CBA/CaJ mice utilizing different age groups and measuring their ABR and DPOAE thresholds, as well as DPOAE amplitudes. The elevated thresholds and reduced amplitudes seen in the older animals compared to the young adult mice are key characteristics of mammalian ARHL. Moreover, correlations found between Cx30 and Cx43 expression and the diminished hearing ability of older animals implicate a relationship between decreases in connexin expression and presbycusis. Significant downregulation of connexin genes and proteins between the age groups, specifically Cx30 and Cx43, was also observed. Changes in connexin expression for other age-related diseases and disorders have previously been reported. For example, researchers have found Cx43 expression decreased with age in rat aortic endothelium, bladder, and bone-marrow. [71-73] Tajima et al. (2020) performed western blot experiments, showing that Cx30, along with Cx26, significantly decreased in C57BL/6J mice at 32 weeks compared with mice at 4 weeks of age. [74] It has also been seen that total deletion of Cx30 in a transgenic mouse model can intensify ARHL, including elevated inflammation and cochlear damage. [75] Moreover, a study from Teubner et al. (2003) showed that in Cx30 knockout mice, the endocochlear potential and auditory hair cells

started to degenerate via cell apoptosis. It was hypothesized this was likely due to a decrease in the endolymphatic K^+ concentration. [76] The previous literature has shown results similar to the ones found in our current study – connexin expression changes with age in various regions in the body.

4.2 Connexins and Kir4.1

Based on our novel findings, changes in expression of Kir4.1 followed a similar pattern to that of Cx30 and Cx43 with aging and aldosterone-treatment. These results are consistent with previous studies done by Liu et at. (2019) who found that Kir4.1 showed decreased expression in aged human cochleae. [77] Consistent with this, in the present study, mice treated with aldosterone displayed increased expression of all three proteins relative to old animals. While not all regions saw equivalent increases for Kir4.1, Cx30, and Cx43 expression levels compared to the young adult animals, some regions did manage to reach and even surpass those levels. These included Cx30 protein expression in the OC, SV, and SGN at all three turns; Cx43 expression in the SGN at the mid and basal turns; and Kir4.1 in the SV and SGN for all three turns, and the OC in the basal turn. The relationships between Kir4.1 and connexins are hypothesized to be connected to their roles in generating the endocochlear potential and maintain homeostasis of cochlear fluids. A study from Chen et al. (2020) has shown that in Cx30 knockout mice, Kir4.1 (KCNJ10) was significantly downregulated in the SV. [26] It has also been seen that in a double knockout model of Cx30 and Cx43, there was impaired potassium clearance during synaptic activity. [78] Moreover, Kir currents were depleted in astrocytes after carbenoxolone, a non-specific connexin inhibitor, was applied to satellite oligodendrocytes. [79] It is possible that a downregulation of both connexins and Kir4.1 could lead to 1) a reduction or even absence of the EP and 2) an accumulation of extracellular K^+ ions around hair cells which can lead to hearing loss and deafness.

Further research should be done to confirm this hypothesis and accompanying mechanisms. Examples of potential experiments include utilizing a mouse model that does show EP changes with age, such as C57BL/6. The effects on connexins on EP can be measured with whole cell patch- clamp experiments comparing young control, old control, aldosterone-treated old, and connexin-knockout mice. Moreover, the detection of K^+ ions can be done utilizing K^+ fluorescent indictors such as a thallium flux assay.

4.3 Aldosterone Exhibits Protective Effects on Connexin Expression

Since connexin proteins are involved in other age-related pathologies, they are appealing therapeutic targets to prevent or even reverse key aspects of these disorders. A potential component of a treatment targeting connexins, hopefully to alleviate some effects of ARHL, is aldosterone therapy. Previously published papers from our lab have shown that aldosterone is a good candidate for treating ARHL because it lowers physiological and behavioral hearing thresholds, prevents apoptosis in spiral ganglion neurons, and can slow down the progression of ARHL and some of its biomarker changes. [53, 54, 56, 57] In the present study, we found that mice who were given aldosterone for a 4-month treatment period had significantly higher levels of Cx30 in all regions and turns of the cochlea compared to old, comparison animals. Moreover, protein expression of Cx43 and Kir4.1 were also higher in aldosterone-treated mice relative to these old, untreated mice. These results are parallel to the *in vitro* findings where we treated cell lines with aldosterone for 24 hours, which increased the gene expression of Cx30 and Cx43. Furthermore, connexin gene expression was boosted to levels significantly greater than the control group following 24-hour combination treatment of H_2O_2 and aldosterone. On the other hand, RT-qPCR experiments showed that gene expression for *Cx30* and *Cx43* in mice did not change significantly; thus, implying that aldosterone triggers post-translations modification (PTM) in *Cx* proteins. PTMs such as

phosphorylation, ubiquination, and methylation have been shown to regulate multiple characteristics of connexins including synthesis, protein-protein interactions, and trafficking. [80, 81] It has also been seen that *Cx43* becomes ubiquitinylated when cells are under stressful conditions, which leads to an uptick in pre-autophagosome proteins such as Atg5 to form autophagosomes. As a result of this regulated autophagy, there is a protective effect on the stressed cells. [82] Conversely, PTMs have been seen to affect connexins and the development of gap junctions in a negative manner. Thévenin et al. (2013) reported how PKC-dependent phosphorylation, which triggered activation of the MAPK pathway, downregulated gap junction ion channels and reduced the half-life of Cx43. [83] Ubiquination has also been shown to lead to degradation of Cx43 by the proteasome. [84, 85] For example, the initiation of ubiquitin-mediated degradation of Cx43 using 12-O-tetradecanoylphorbol 13-actetate (TPA) was inhibited by proteasomal inhibitors. [85] Moreover, it has previously been shown that aldosterone reversed downregulation of mineralocorticoid receptors and prevented downregulation of Na^+-K^+-$2Cl^-$ cotransporter protein (NKCC1) via PTM ubiquitination. [86] To the best of our knowledge, there are no studies that have explored aldosterone's effect on connexin expression via PTMs. This is an area that will require further research.

Aldosterone is also naturally produced in the human body, making the administration of it for humans safe with the proper dose controls. Hypertension is a potential drawback to administering this treatment if serum levels are not carefully monitored; however, when aldosterone was administered to aging CBA/CaJ mice there was no elevation in their blood pressure throughout the entire treatment time. [54] In other physiological systems, previous research has shown that aldosterone modulates the expression of connexins, specifically Cx43. [87] For example, Suzuki et al. (2009) treated rat ventricular myocytes with aldosterone and

noticed an upregulation in Cx43 mRNA gene expression. This is parallel to the results we found in our RT-qPCR experiments in the present study. Similar results were seen with Kir4.1 expression. In MIO-M1 cells derived from the retina, aldosterone treatment significantly upregulated Kir4.1 mRNA as well as protein expression. [39] Another study from Allingham (2018) also showed increased Kir4.1 staining in the inner nuclear layer, outer plexiform layer, and inner plexiform layer in the retina in aldosterone-treated mice. [88] These findings are analogous to the results seen in our gene and protein expression experiments.

The biological mechanisms underlying the modulation of connexin and Kir4.1 due to aldosterone therapy is still a novel area of research. One explanation is that aldosterone binds to intracellular receptors that are able to control the transcription of genes, including Cx43. [80] A mineralocorticoid receptor (MR)-hormone complex can activate transcription of a gene by binding to a transcription regulatory element. In the rat cardiac Cx43 gene, there is a site for hormone response elements that can bind with the MR-hormone complex leading to the upregulation of Cx43 after aldosterone is introduced. [89] Another potential mechanism involves the protein kinase C (PKC) and/or mitogen-activated protein kinase (MAPK) pathway. Multiple studies have shown that that aldosterone activates the PKC and MAPK pathways which connexins, specifically Cx43, have also been seen being phosphorylated in those pathways. [87, 90, 91] The relationship between the MAPK and PKC pathways with Kir4.1 is still being researched, but currently it seems that the MAPK pathway can induce Kir4.1 since it is colocalized with aquaporin-4 (AQP4) in the cochlea and it has been seen that MAPK induces AQP4 expression in astrocytes. [92, 93] Also, note that gene expression studies have revealed a role for AQP4 channel changes in mammalian ARHL [94]. It will be important to consider these findings from other systems when designing

new studies of the auditory system and conducting further experiments observing the therapeutic effects of aldosterone on connexin expression in the cochlea and central auditory system.

4.4 Other Mechanisms Involvement in Modulating Connexin Expression

4.4.1 ROS Production

The differences in expression for the connexin proteins could be caused by a myriad of mechanisms. Investigating the biological mechanisms driving these changes is our next, continuing step to more fully understand the roles that connexins play in ARHL. A potential related factor is the increased levels of reactive oxygen species (ROS) associated with aging. Martinez and Saez (2000) found that increases in ROS production are associated with changes in expression and function of Cx43 gap junction channels in rat cortical astrocytes. [36] H_2O_2 is an abundant ROS that causes oxidative stress in the cochlea; thus, leading to cell damage in the inner ear. [95] In the present study, H_2O_2 was used to treat cells to model the aged cochlea to a first approximation. Our results showed a decrease in Cx30 and Cx43 gene and protein expression after 24-hour treatment with hydrogen peroxide. This decrease in expression parallels what was seen in our *in vivo* ARHL animal studies. The effects of this interaction between ROS and connexins in relation to ARHL still has to be studied to see what molecular pathways, cells, and other facets of the cochlea are being altered.

4.4.2 Autophagy

Another possible explanation for the age changes in Cx30 and Cx43 expression may have to do with alterations in the autophagy pathway. Autophagy is a self-preservation metabolic pathway (relatively under-studied in the aging auditory system) that performs multiple important roles in cell survival and maintaining homeostasis in the body at the cellular level. For instance, it has been seen that autophagic promoters, such as rapamycin, may be potential therapeutic agents

for ARHL. [34] There have been no studies published yet to our knowledge, investigating the connection between autophagy and connexins in the inner ear. However, there have been publications researching this connection in other systems of the body. Wang et al. (2017) found that Cx43 expression was restored following hyperglycemia-induced apoptosis though the stimulation of the autophagy pathway. [96] Other studies have shown that autophagy altered connexin expression in the rat brain, cardiomyocytes, and HeLa cells. [96-98] Conversely, it is also hypothesized that connexins regulate the autophagic process by recruiting autophagy-related proteins to the plasma membrane; hence, limiting their readiness for regulating autophagy. [99] Future experiments will be conducted in hopes of finding which cellular and molecular mechanisms are behind the age changes in cochlear connexin expression levels.

Chapter 5: Summary and Conclusions

From our study, new connections between connexins, particularly Cx30 and Cx43, and ARHL have been revealed. *In vitro* GeneChip and qPCR experiments provided evidence that Cx30 and Cx43 gene expression decreases with age. These findings are consistent with the results from our *in vivo* immunohistochemistry experiments that also showed decreases in both connexin protein expressions with age. Since our *in vivo* samples did not show changes in gene expression, the aldosterone effects taken together indicate that these therapeutic changes involve cochlear post-translational protein modifications. ABR and DPOAEs from the animals utilized confirmed ARHL was occurring for our old animal groups. Moreover, it was also observed that Kir4.1 decreased with age. The decrease in Kir4.1, Cx30, and Cx43 protein expression in old animals was minimized with long-term aldosterone treatment. Mice that were given aldosterone for a four-month period showed Cx30, Cx43, Kir4.1 protein levels higher than old, comparison mice that received a saline placebo. Furthermore, ABR threshold levels of mice treated with aldosterone showed a protective effect, especially at higher frequencies. The thresholds barely shifted throughout the four months for the aldosterone-treated mice, while the old, untreated mice showed shifts that are characteristic of classic ARHL. Our novel findings indicate that aldosterone provides protective effects against ARHL and helps conserve Cx30, Cx43, and Kir4.1 protein levels.

In conclusion, our findings indicate that Cx30, Cx43, and Kir4.1 work in conjunction to preserve hearing with aging and should be considered when developing therapeutic cocktails or multi-faceted therapy approaches for ARHL. Indeed, the aging mouse model employed here showed that aldosterone hinders the development of key aspects and biomarkers of presbycusis.

More research is required to pinpoint which pathways are directly involved in the modulation of cochlear connexins and potassium channels such as Kir4.1, by aldosterone. So, understanding what cellular pathways are involved in the progression of ARHL is critical when developing medications and treatment plans for this highly-prevalent neurodegenerative disorder of our elderly population.

References

1. Orellana, J., Giaume, C., & Sa?ez, J. (2011). Role of Connexin Hemichannels in Neurodegeneration. In. https://doi.org/10.5772/28054

2. Moore, B. C. (2007). *Cochlear hearing loss: physiological, psychological and technical issues*. John Wiley & Sons.

3. Martinez, A. D., Acuna, R., Figueroa, V., Maripillan, J., & Nicholson, B. (2009). Gap-junction channels dysfunction in deafness and hearing loss. *Antioxid Redox Signal*, *11*(2), 309-322. https://doi.org/10.1089/ars.2008.2138

4. Watson, N., Ding, B., Zhu, X., & Frisina, R. D. (2017). Chronic inflammation - inflammaging - in the ageing cochlea: A novel target for future presbycusis therapy. *Ageing Res Rev*, *40*, 142-148. https://doi.org/10.1016/j.arr.2017.10.002

5. *Age-Related Hearing Loss*. (2022). National Institute on Deafness and Other Communcation Disorders. https://www.nidcd.nih.gov/health/age-related-hearing-loss.
6. Gates, G. A., & Mills, J. H. (2005). Presbycusis. *Lancet*, *366*(9491), 1111-1120. https://doi.org/10.1016/S0140-6736(05)67423-5

7. Wang, J., & Puel, J. L. (2020). Presbycusis: An Update on Cochlear Mechanisms and Therapies. *J Clin Med*, *9*(1). https://doi.org/10.3390/jcm9010218

8. Fetoni, A. R., Picciotti, P. M., Paludetti, G., & Troiani, D. (2011). Pathogenesis of presbycusis in animal models: a review. *Exp Gerontol*, *46*(6), 413-425. https://doi.org/10.1016/j.exger.2010.12.003

9. Møller, A. R. (2012). *Hearing: anatomy, physiology, and disorders of the auditory system*. Plural Publishing.

10. Khan, S., & Chang, R. (2013). Anatomy of the vestibular system: a review. *NeuroRehabilitation*, *32*(3), 437-443. https://doi.org/10.3233/NRE-130866

11. Gelfand, S. A. (2010). *Hearing an introduction to psychological and physiological acoustics* (5th ed.). Informa Healthcare,. http://www.usf.eblib.com/patron/FullRecord.aspx?p=485593

12. Dallos, P., Popper, A. N., & Fay, R. R. (1996). *The Cochlea*. Springer New York : Imprint : Springer,. http://ezproxy.lib.usf.edu/login?url=http://link.springer.com/10.1007/978-1-4612-0757-3

13. Liu, H., Li, Y., Chen, L., Zhang, Q., Pan, N., Nichols, D. H., Zhang, W. J., Fritzsch, B., & He, D. Z. Z. (2016). Organ of Corti and Stria Vascularis: Is there an Interdependence for Survival? *PloS one*, *11*(12), e0168953-e0168953. https://doi.org/10.1371/journal.pone.0168953

14. Patuzzi, R. (2011). Ion flow in stria vascularis and the production and regulation of cochlear endolymph and the endolymphatic potential. *Hear Res*, *277*(1-2), 4-19. https://doi.org/10.1016/j.heares.2011.01.010

15. Schuknecht, H. F., Watanuki, K., Takahashi, T., Belal, A. A., Jr., Kimura, R. S., Jones, D. D., & Ota, C. Y. (1974). Atrophy of the stria vascularis, a common cause for hearing loss. *Laryngoscope*, *84*(10), 1777-1821. https://doi.org/10.1288/00005537-197410000-00012

16. Kopecky, B., & Fritzsch, B. (2011). Regeneration of Hair Cells: Making Sense of All the Noise. *Pharmaceuticals (Basel)*, *4*(6), 848-879. https://doi.org/10.3390/ph4060848

17. Hu, Z., Komal, F., Singh, A., & Deng, M. (2021). Generation of a Spiral Ganglion Neuron Degeneration Mouse Model. *Front Cell Dev Biol*, *9*, 761847. https://doi.org/10.3389/fcell.2021.761847

18. Kelly, J. J., Abitbol, J. M., Hulme, S., Press, E. R., Laird, D. W., & Allman, B. L. (2019). The connexin 30 A88V mutant reduces cochlear gap junction expression and confers long-term protection against hearing loss. *J Cell Sci*, *132*(2). https://doi.org/10.1242/jcs.224097

19. Lefebvre, P. P., & Van De Water, T. R. (2000). Connexins, hearing and deafness: clinical aspects of mutations in the connexin 26 gene. *Brain Res Brain Res Rev*, *32*(1), 159-162. https://doi.org/10.1016/s0165-0173(99)00075-2

20. Liu, W. J., & Yang, J. (2015). Preferentially regulated expression of connexin 43 in the developing spiral ganglion neurons and afferent terminals in post-natal rat cochlea. *Eur J Histochem*, *59*(1), 2464. https://doi.org/10.4081/ejh.2015.2464

21. Qu, Y., Tang, W., Dahlke, I., Ding, D., Salvi, R., Sohl, G., Willecke, K., Chen, P., & Lin, X. (2007). Analysis of connexin subunits required for the survival of vestibular hair cells. *J Comp Neurol*, *504*(5), 499-507. https://doi.org/10.1002/cne.21459

22. Tang, W., Zhang, Y., Chang, Q., Ahmad, S., Dahlke, I., Yi, H., Chen, P., Paul, D. L., & Lin, X. (2006). Connexin29 is highly expressed in cochlear Schwann cells, and it is required for the normal development and function of the auditory nerve of mice. *J Neurosci*, *26*(7), 1991-1999. https://doi.org/10.1523/JNEUROSCI.5055-05.2006

23. Verselis, V. K. (2019). Connexin hemichannels and cochlear function. *Neurosci Lett*, *695*, 40-45. https://doi.org/10.1016/j.neulet.2017.09.020

24. Erbe, C. B., Harris, K. C., Runge-Samuelson, C. L., Flanary, V. A., & Wackym, P. A. (2004). Connexin 26 and connexin 30 mutations in children with nonsyndromic hearing loss. *Laryngoscope*, *114*(4), 607-611. https://doi.org/10.1097/00005537-200404000-00003

25. Park, H. J., Hahn, S. H., Chun, Y. M., Park, K., & Kim, H. N. (2000). Connexin26 mutations associated with nonsyndromic hearing loss. *Laryngoscope*, *110*(9), 1535-1538. https://doi.org/10.1097/00005537-200009000-00023

26. Chen, B., Xu, H., Mi, Y., Jiang, W., Guo, D., Zhang, J., Zhao, Y., & Tang, W. (2020). Mechanisms of hearing loss and cell death in the cochlea of connexin mutant mice. *Am J Physiol Cell Physiol*, *319*(3), C569-C578. https://doi.org/10.1152/ajpcell.00483.2019

27. Lin, L., Wang, Y. F., Wang, S. Y., Liu, S. F., Yu, Z., Xi, L., & Li, H. W. (2013). Ultrastructural pathological changes in the cochlear cells of connexin 26 conditional knockout mice. *Mol Med Rep*, *8*(4), 1029-1036. https://doi.org/10.3892/mmr.2013.1614

28. Wu, X., Zhang, W., Li, Y., & Lin, X. (2019). Structure and Function of Cochlear Gap Junctions and Implications for the Translation of Cochlear Gene Therapies. *Front Cell Neurosci*, *13*, 529. https://doi.org/10.3389/fncel.2019.00529

29. Le, H. T., Sin, W. C., Lozinsky, S., Bechberger, J., Vega, J. L., Guo, X. Q., Saez, J. C., & Naus, C. C. (2014). Gap junction intercellular communication mediated by connexin43 in astrocytes is essential for their resistance to oxidative stress. *J Biol Chem*, *289*(3), 1345-1354. https://doi.org/10.1074/jbc.M113.508390

30. Lukashkina, V. A., Levic, S., Lukashkin, A. N., Strenzke, N., & Russell, I. J. (2017). A connexin30 mutation rescues hearing and reveals roles for gap junctions in cochlear amplification and micromechanics [Article]. *Nature Communications*, *8*. https://doi.org/10.1038/ncomms14530

31. Liu, X., & Yan, D. (2007). Ageing and hearing loss. *The Journal of Pathology*, *211*(2), 188-197. https://doi.org/10.1002/path.2102

32. Jagger, D. J., & Forge, A. (2015). Connexins and gap junctions in the inner ear--it's not just about K(+) recycling. *Cell Tissue Res*, *360*(3), 633-644. https://doi.org/10.1007/s00441-014-2029-z

33. Jones, S. A., Lancaster, M. K., & Boyett, M. R. (2004). Ageing-related changes of connexins and conduction within the sinoatrial node. *J Physiol*, *560*(Pt 2), 429-437. https://doi.org/10.1113/jphysiol.2004.072108

34. Fu, X., & Chai, R. (2019). Regulation of autophagy: a promising therapeutic target for the treatment of hearing loss. *Journal of Bio-X Research*, *2*(2). https://journals.lww.com/jbioxresearch/Fulltext/2019/06000/Regulation_of_autophagy__a_promising_therapeutic.1.aspx

35. Fukuda, T., Ikejima, K., Hirose, M., Takei, Y., Watanabe, S., & Sato, N. (2000). Taurine preserves gap junctional intercellular communication in rat hepatocytes under oxidative stress. *J Gastroenterol*, *35*(5), 361-368. https://doi.org/10.1007/s005350050361

36. Martinez, A. D., & Saez, J. C. (2000). Regulation of astrocyte gap junctions by hypoxia-reoxygenation. *Brain Res Brain Res Rev*, *32*(1), 250-258. https://doi.org/10.1016/s0165-0173(99)00086-7

37. Tan, M. L. L., Kwong, H. L., Ang, C. C., Tey, H. L., Lee, J. S. S., & Becker, D. L. (2021). Changes in connexin 43 in inflammatory skin disorders: Eczema, psoriasis, and Steven-Johnson syndrome/toxic epidermal necrolysis. *Health Sci Rep*, *4*(1), e247. https://doi.org/10.1002/hsr2.247

38. Zhang, Z., Yao, W., Yuan, D., Huang, F., Liu, Y., Luo, G., & Hei, Z. (2020). Effects of Connexin 32-Mediated Lung Inflammation Resolution During Liver Ischemia Reperfusion. *Dig Dis Sci*, *65*(10), 2914-2924. https://doi.org/10.1007/s10620-019-06020-8

39. Zhao, M., Valamanesh, F., Celerier, I., Savoldelli, M., Jonet, L., Jeanny, J. C., Jaisser, F., Farman, N., & Behar-Cohen, F. (2010). The neuroretina is a novel mineralocorticoid target: aldosterone up-regulates ion and water channels in Muller glial cells. *FASEB J*, *24*(9), 3405-3415. https://doi.org/10.1096/fj.09-154344

40. Papanikolaou, M., Lewis, A., & Butt, A. M. (2019). Glial and neuronal expression of the Inward Rectifying Potassium Channel Kir7.1 in the adult mouse brain. *J Anat*, *235*(5), 984-996. https://doi.org/10.1111/joa.13048

41. Bazard, P., Frisina, R. D., Acosta, A. A., Dasgupta, S., Bauer, M. A., Zhu, X., & Ding, B. (2021). Roles of Key Ion Channels and Transport Proteins in Age-Related Hearing Loss. *Int J Mol Sci*, *22*(11). https://doi.org/10.3390/ijms22116158

42. Chen, J., & Zhao, H. B. (2014). The role of an inwardly rectifying K(+) channel (Kir4.1) in the inner ear and hearing loss. *Neuroscience*, *265*, 137-146. https://doi.org/10.1016/j.neuroscience.2014.01.036

43. Locher, H., de Groot, J. C., van Iperen, L., Huisman, M. A., Frijns, J. H., & Chuva de Sousa Lopes, S. M. (2015). Development of the stria vascularis and potassium regulation in the human fetal cochlea: Insights into hereditary sensorineural hearing loss. *Dev Neurobiol*, *75*(11), 1219-1240. https://doi.org/10.1002/dneu.22279

44. Wangemann, P., & Schacht, J. (1996). Homeostatic Mechanisms in the Cochlea. In P. Dallos, A. N. Popper, & R. R. Fay (Eds.), *The Cochlea* (pp. 130-185). Springer New York. https://doi.org/10.1007/978-1-4612-0757-3_3

45. Kelly, J., Forge, A., & Jagger, D. (2011). Development of gap junctional intercellular communication within the lateral wall of the rat cochlea. *Neuroscience*, *180*, 360-369.

46. Liu, Y. P., & Zhao, H. B. (2008). Cellular characterization of Connexin26 and Connnexin30 expression in the cochlear lateral wall. *Cell Tissue Res*, *333*(3), 395-403. https://doi.org/10.1007/s00441-008-0641-5

47. Hibino, H., Horio, Y., Fujita, A., Inanobe, A., Doi, K., Gotow, T., Uchiyama, Y., Kubo, T., & Kurachi, Y. (1999). Expression of an inwardly rectifying K+ channel, Kir4. 1, in satellite cells of rat cochlear ganglia. *American Journal of Physiology-Cell Physiology*, *277*(4), C638-C644.

48. Bockenhauer, D., Feather, S., Stanescu, H. C., Bandulik, S., Zdebik, A. A., Reichold, M., Tobin, J., Lieberer, E., Sterner, C., & Landoure, G. (2009). Epilepsy, ataxia, sensorineural deafness, tubulopathy, and KCNJ10 mutations. *New England Journal of Medicine*, *360*(19), 1960-1970.

49. Scholl, U. I., Choi, M., Liu, T., Ramaekers, V. T., Häusler, M. G., Grimmer, J., Tobe, S. W., Farhi, A., Nelson-Williams, C., & Lifton, R. P. (2009). Seizures, sensorineural deafness, ataxia, mental retardation, and electrolyte imbalance (SeSAME syndrome) caused by mutations in KCNJ10. *Proceedings of the National Academy of Sciences*, *106*(14), 5842-5847.

50. Marcus, D. C., Wu, T., Wangemann, P., & Kofuji, P. (2002). KCNJ10 (Kir4. 1) potassium channel knockout abolishes endocochlear potential. *American Journal of Physiology-Cell Physiology*, *282*(2), C403-C407.

51. Neusch, C., Rozengurt, N., Jacobs, R. E., Lester, H. A., & Kofuji, P. (2001). Kir4. 1 potassium channel subunit is crucial for oligodendrocyte development and in vivo myelination. *Journal of Neuroscience*, *21*(15), 5429-5438.

52. Rozengurt, N., Lopez, I., Chiu, C.-S., Kofuji, P., Lester, H. A., & Neusch, C. (2003). Time course of inner ear degeneration and deafness in mice lacking the Kir4. 1 potassium channel subunit. *Hearing Research*, *177*(1-2), 71-80.

53. Ding, B., Frisina, R. D., Zhu, X., Sakai, Y., Sokolowski, B., & Walton, J. P. (2014). Direct control of Na(+)-K(+)-2Cl(-)-cotransport protein (NKCC1) expression with aldosterone. *Am J Physiol Cell Physiol*, *306*(1), C66-75. https://doi.org/10.1152/ajpcell.00096.2013

54. Halonen, J., Hinton, A. S., Frisina, R. D., Ding, B., Zhu, X., & Walton, J. P. (2016). Long-term treatment with aldosterone slows the progression of age-related hearing loss. *Hear Res*, *336*, 63-71. https://doi.org/10.1016/j.heares.2016.05.001

55. Trune, D. R., & Kempton, J. B. (2001). Aldosterone and prednisolone control of cochlear function in MRL/MpJ-Faslpr autoimmune mice. *Hearing Research*, *155*(1), 9-20. https://doi.org/https://doi.org/10.1016/S0378-5955(01)00240-4

56. Frisina, R. D., Ding, B., Zhu, X., & Walton, J. P. (2016). Age-related hearing loss: prevention of threshold declines, cell loss and apoptosis in spiral ganglion neurons. *Aging (Albany NY)*, *8*(9), 2081-2099. https://doi.org/10.18632/aging.101045

57. Tadros, S. F., Frisina, S. T., Mapes, F., Frisina, D. R., & Frisina, R. D. (2005). Higher serum aldosterone correlates with lower hearing thresholds: a possible protective hormone against presbycusis. *Hear Res*, *209*(1-2), 10-18. https://doi.org/10.1016/j.heares.2005.05.009

58. Tadros, S. F., D'Souza, M., Zettel, M. L., Zhu, X., Lynch-Erhardt, M., & Frisina, R. D. (2007). Serotonin 2B receptor: upregulated with age and hearing loss in mouse auditory system. *Neurobiol Aging*, *28*(7), 1112-1123. https://doi.org/10.1016/j.neurobiolaging.2006.05.021

59. Tadros, S. F., D'Souza, M., Zettel, M. L., Zhu, X., Waxmonsky, N. C., & Frisina, R. D. (2007). Glutamate-related gene expression changes with age in the mouse auditory midbrain. *Brain Res*, *1127*(1), 1-9. https://doi.org/10.1016/j.brainres.2006.09.081

60. Tadros, S. F., D'Souza, M., Zhu, X., & Frisina, R. D. (2014). Gene expression changes for antioxidants pathways in the mouse cochlea: relations to age-related hearing deficits. *PloS one*, *9*(2), e90279. https://doi.org/10.1371/journal.pone.0090279

61. Williamson, T. T., Zhu, X., Walton, J. P., & Frisina, R. D. (2015). Auditory brainstem gap responses start to decline in mice in middle age: a novel physiological biomarker for age-related hearing loss. *Cell Tissue Res*, *361*(1), 359-369. https://doi.org/10.1007/s00441-014-2003-9

62. Frisina, R. D., & Zhu, X. (2010). Auditory sensitivity and the outer hair cell system in the CBA mouse model of age-related hearing loss. *Open Access Anim Physiol*, *2*, 9-16. https://doi.org/10.2147/OAAP.S7202

63. Bazard, P., Ding, B., Chittam, H. K., Zhu, X., Parks, T. A., Taylor-Clark, T. E., Bhethanabotla, V. R., Frisina, R. D., & Walton, J. P. (2020). Aldosterone up-regulates voltage-gated potassium currents and NKCC1 protein membrane fractions. *Sci Rep*, *10*(1), 15604. https://doi.org/10.1038/s41598-020-72450-4

64. Benkafadar, N., Francois, F., Affortit, C., Casas, F., Ceccato, J. C., Menardo, J., Venail, F., Malfroy-Camine, B., Puel, J. L., & Wang, J. (2019). ROS-Induced Activation of DNA Damage Responses Drives Senescence-Like State in Postmitotic Cochlear Cells: Implication for Hearing Preservation. *Mol Neurobiol*, *56*(8), 5950-5969. https://doi.org/10.1007/s12035-019-1493-6

65. Clerici, W. J., DiMartino, D. L., & Prasad, M. R. (1995). Direct effects of reactive oxygen species on cochlear outer hair cell shape in vitro. *Hear Res*, *84*(1-2), 30-40. https://doi.org/10.1016/0378-5955(95)00010-2

66. Ding, B., Walton, J. P., Zhu, X., & Frisina, R. D. (2018). Age-related changes in Na, K-ATPase expression, subunit isoform selection and assembly in the stria vascularis lateral wall of mouse cochlea. *Hear Res*, *367*, 59-73. https://doi.org/10.1016/j.heares.2018.07.006

67. Williamson, T. T., Ding, B., Zhu, X., & Frisina, R. D. (2019). Hormone replacement therapy attenuates hearing loss: Mechanisms involving estrogen and the IGF-1 pathway. *Aging Cell*, *18*(3), e12939. https://doi.org/10.1111/acel.12939

68. Bustin, S. A., Benes, V., Nolan, T., & Pfaffl, M. W. (2005). Quantitative real-time RT-PCR--a perspective. *J Mol Endocrinol*, *34*(3), 597-601. https://doi.org/10.1677/jme.1.01755

69. Ahmad Waza, A., Ahmad Bhat, S., Ul Hussain, M., & Ganai, B. A. (2018). Connexin 43 and ATP-sensitive potassium channels crosstalk: a missing link in hypoxia/ischemia stress. *Cell Tissue Res*, *371*(2), 213-222. https://doi.org/10.1007/s00441-017-2736-3

70. Du, M., Li, J., Chen, L., Yu, Y., & Wu, Y. (2018). Astrocytic Kir4.1 channels and gap junctions account for spontaneous epileptic seizure. *PLoS Comput Biol*, *14*(3), e1005877. https://doi.org/10.1371/journal.pcbi.1005877

71. Asumda, F. Z., & Chase, P. B. (2011). Age-related changes in rat bone-marrow mesenchymal stem cell plasticity. *BMC Cell Biol*, *12*, 44. https://doi.org/10.1186/1471-2121-12-44

72. Song, S. H., Joo, H. T., Cho, H. W., Hwang, H. W., Lee, K. H., & Kim, D. K. (2011). Sex- and age-related changes in connexin 43 expression in normal rat bladder. *Int Neurourol J*, *15*(1), 25-28. https://doi.org/10.5213/inj.2011.15.1.25

73. Yeh, H. I., Chang, H. M., Lu, W. W., Lee, Y. N., Ko, Y. S., Severs, N. J., & Tsai, C. H. (2000). Age-related alteration of gap junction distribution and connexin expression in rat aortic endothelium. *J Histochem Cytochem*, *48*(10), 1377-1389. https://doi.org/10.1177/002215540004801008

74. Tajima, S., Danzaki, K., Ikeda, K., & Kamiya, K. (2020). Degradation and modification of cochlear gap junction proteins in the early development of age-related hearing loss. *Exp Mol Med*, *52*(1), 166-175. https://doi.org/10.1038/s12276-020-0377-1

75. Paciello, F., Zorzi, V., Raspa, M., Scavizzi, F., Grassi, C., Mammano, F., & Fetoni, A. R. (2022). Connexin 30 deletion exacerbates cochlear senescence and age-related hearing loss. *Front Cell Dev Biol*, *10*, 950837. https://doi.org/10.3389/fcell.2022.950837

76. Teubner, B., Michel, V., Pesch, J., Lautermann, J., Cohen-Salmon, M., Sohl, G., Jahnke, K., Winterhager, E., Herberhold, C., Hardelin, J. P., Petit, C., & Willecke, K. (2003). Connexin30 (Gjb6)-deficiency causes severe hearing impairment and lack of endocochlear potential. *Hum Mol Genet*, *12*(1), 13-21. https://doi.org/10.1093/hmg/ddg001

77. Liu, T., Li, G., Noble, K. V., Li, Y., Barth, J. L., Schulte, B. A., & Lang, H. (2019). Age-dependent alterations of Kir4.1 expression in neural crest-derived cells of the mouse and human cochlea. *Neurobiol Aging*, *80*, 210-222. https://doi.org/10.1016/j.neurobiolaging.2019.04.009

78. Pannasch, U., Vargová, L., Reingruber, J., Ezan, P., Holcman, D., Giaume, C., Syková, E., & Rouach, N. (2011). Astroglial networks scale synaptic activity and plasticity. *Proc Natl Acad Sci U S A*, *108*(20), 8467-8472. https://doi.org/10.1073/pnas.1016650108

79. Battefeld, A., Klooster, J., & Kole, M. H. (2016). Myelinating satellite oligodendrocytes are integrated in a glial syncytium constraining neuronal high-frequency activity. *Nat Commun*, *7*, 11298. https://doi.org/10.1038/ncomms11298

80. Axelsen, L., Calloe, K., Holstein-Rathlou, N.-H., & Nielsen, M. (2013). Managing the complexity of communication: regulation of gap junctions by post-translational modification [Review]. *Frontiers in Pharmacology*, *4*. https://doi.org/10.3389/fphar.2013.00130

81. Aasen, T., Johnstone, S., Vidal-Brime, L., Lynn, K. S., & Koval, M. (2018). Connexins: Synthesis, Post-Translational Modifications, and Trafficking in Health and Disease. *Int J Mol Sci*, *19*(5). https://doi.org/10.3390/ijms19051296

82. Bejarano, E., Yuste, A., Patel, B., Stout, R. F., Jr., Spray, D. C., & Cuervo, A. M. (2014). Connexins modulate autophagosome biogenesis. *Nat Cell Biol*, *16*(5), 401-414. https://doi.org/10.1038/ncb2934

83. Thévenin, A. F., Kowal, T. J., Fong, J. T., Kells, R. M., Fisher, C. G., & Falk, M. M. (2013). Proteins and mechanisms regulating gap-junction assembly, internalization, and degradation. *Physiology (Bethesda, Md.)*, 28(2), 93–116. https://doi.org/10.1152/physiol.00038.2012

84. Johnstone, S. R., Billaud, M., Lohman, A. W., Taddeo, E. P., & Isakson, B. E. (2012). Posttranslational modifications in connexins and pannexins. *The Journal of membrane biology*, *245*(5-6), 319–332. https://doi.org/10.1007/s00232-012-9453-3

85. Leithe, E., & Rivedal, E. (2004). Ubiquitination and down-regulation of gap junction protein connexin-43 in response to 12-O-tetradecanoylphorbol 13-acetate treatment. *The Journal of biological chemistry*, *279*(48), 50089–50096. https://doi.org/10.1074/jbc.M402006200

86. Bazard, P., Pineros, J., Acosta, A. A., Thivierge, M., Paganella, L. R., Zucker, S., Mannering, F. L., Modukuri, S., Zhu, X., Frisina, R. D., & Ding, B. (2022). Post-Translational Modifications and Age-related Hearing Loss. *Hearing Research*, 108625. https://doi.org/https://doi.org/10.1016/j.heares.2022.108625

87. Suzuki, S., Ohkusa, T., Sato, T., Yoshida, M., Yasui, K., Miwa, K., Lee, J. K., Yano, M., Kodama, I., & Matsuzaki, M. (2009). Effects of aldosterone on Cx43 gap junction expression in neonatal rat cultured cardiomyocytes. *Circ J*, *73*(8), 1504-1512. https://doi.org/10.1253/circj.cj-08-1065

88. Allingham, M. J., Tserentsoodol, N., Saloupis, P., Mettu, P. S., & Cousins, S. W. (2018). Aldosterone Exposure Causes Increased Retinal Edema and Severe Retinopathy Following Laser-Induced Retinal Vein Occlusion in Mice. *Invest Ophthalmol Vis Sci*, *59*(8), 3355-3365. https://doi.org/10.1167/iovs.17-23073

89. Funder, J. W. (1997). Glucocorticoid and mineralocorticoid receptors: biology and clinical relevance. *Annu Rev Med*, *48*, 231-240. https://doi.org/10.1146/annurev.med.48.1.231

90. Alzamora, R., Brown, L. R., & Harvey, B. J. (2007). Direct binding and activation of protein kinase C isoforms by aldosterone and 17β-estradiol. *Molecular Endocrinology*, *21*(11), 2637-2650.

91. Nimlamool, W., Andrews, R. M., & Falk, M. M. (2015). Connexin43 phosphorylation by PKC and MAPK signals VEGF-mediated gap junction internalization. *Mol Biol Cell*, *26*(15), 2755-2768. https://doi.org/10.1091/mbc.E14-06-1105

92. Eckhard, A., Gleiser, C., Rask-Andersen, H., Arnold, H., Liu, W., Mack, A., Müller, M., Löwenheim, H., & Hirt, B. (2012). Co-localisation of Kir4.1 and AQP4 in rat and human cochleae reveals a gap in water channel expression at the transduction sites of endocochlear K+ recycling routes. *Cell and Tissue Research*, *350*(1), 27-43. https://doi.org/10.1007/s00441-012-1456-y

93. McCoy, E., & Sontheimer, H. (2010). MAPK induces AQP1 expression in astrocytes following injury. *Glia*, *58*(2), 209-217. https://doi.org/10.1002/glia.20916

94. Christensen, N., D'Souza, M., Zhu, X., & Frisina, R. D. (2009). Age-related hearing loss: aquaporin 4 gene expression changes in the mouse cochlea and auditory midbrain. *Brain Res*, *1253*, 27-34. https://doi.org/10.1016/j.brainres.2008.11.070

95. Dehne, N., Lautermann, J., ten Cate, W. J., Rauen, U., & de Groot, H. (2000). In vitro effects of hydrogen peroxide on the cochlear neurosensory epithelium of the guinea pig. *Hear Res*, *143*(1-2), 162-170. https://doi.org/10.1016/s0378-5955(00)00036-8

96. Wang, G. Y., Bi, Y. G., Liu, X. D., Zhao, Y., Han, J. F., Wei, M., & Zhang, Q. Y. (2017). Autophagy was involved in the protective effect of metformin on hyperglycemia-induced cardiomyocyte apoptosis and Connexin43 downregulation in H9c2 cells. *Int J Med Sci*, *14*(7), 698-704. https://doi.org/10.7150/ijms.19800

97. Fong, J. T., Kells, R. M., Gumpert, A. M., Marzillier, J. Y., Davidson, M. W., & Falk, M. M. (2012). Internalized gap junctions are degraded by autophagy. *Autophagy*, *8*(5), 794-811. https://doi.org/10.4161/auto.19390

98. Sun, L., Gao, J., Zhao, M., Jing, X., Cui, Y., Xu, X., Wang, K., Zhang, W., & Cui, J. (2014). The effects of BMSCs transplantation on autophagy by CX43 in the hippocampus following traumatic brain injury in rats. *Neurol Sci*, *35*(5), 677-682. https://doi.org/10.1007/s10072-013-1575-6

99. Iyyathurai, J., Decuypere, J. P., Leybaert, L., D'Hondt, C., & Bultynck, G. (2016). Connexins: substrates and regulators of autophagy. *BMC Cell Biol*, *17 Suppl 1*, 20. https://doi.org/10.1186/s12860-016-0093-9

Appendix A: Copyright Permissions

The following information is permission from John Wiley and Sons for the use of material in Chapter 1.

This Agreement between University of South Florida -- Jennifer Pineros ("You") and John Wiley and Sons ("John Wiley and Sons") consists of your license details and the terms and conditions provided by John Wiley and Sons and Copyright Clearance Center.

License Number	5402560354724
License date	Oct 05, 2022
Licensed Content Publisher	John Wiley and Sons
Licensed Content Publication	Wiley Books
Licensed Content Title	Cochlear Hearing Loss: Physiological, Psychological and Technical Issues, 2nd Edition
Licensed Content Author	Brian C. J. Moore
Licensed Content Date	Nov 1, 2007
Licensed Content Pages	1
Type of use	Dissertation/Thesis
Requestor type	University/Academic
Format	Electronic
Portion	Figure/table
Number of figures/tables	1
Will you be translating?	No
Title	Student
Institution name	University of South Florida
Expected presentation date	Oct 2022
Order reference number	
Portions	Chapter 1, Figure 1.5.

The permission below is from Mary Ann Liebert Inc. for the use of material in Chapter 1.

CCC | Marketplace™

This is a License Agreement between Jennifer Pineros ("User") and Copyright Clearance Center, Inc. ("CCC") on behalf of the Rightsholder identified in the order details below. The license consists of the order details, the Marketplace Order General Terms and Conditions below, and any Rightsholder Terms and Conditions which are included below.

All payments must be made in full to CCC in accordance with the Marketplace Order General Terms and Conditions below.

Order Date	06-Oct-2022	Type of Use	Republish in a thesis/dissertation
Order License ID	1276524-1	Publisher	MARY ANN/LIEBERT, INC. PUBLISHERS
ISSN	1523-0864	Portion	Image/photo/illustration

LICENSED CONTENT

Publication Title	Antioxidants & redox signaling	Rightsholder	Mary Ann Liebert Inc.
Article Title	Gap-junction channels dysfunction in deafness and hearing loss.	Publication Type	Journal
		Start Page	309
Author/Editor	Mary Ann Liebert, Inc.	End Page	322
Date	01/01/1999	Issue	2
Language	English	Volume	11
Country	United States of America		

REQUEST DETAILS

Portion Type	Image/photo/illustration	Distribution	Worldwide
Number of images / photos / illustrations	1	Translation	Original language of publication
		Copies for the disabled?	No
Format (select all that apply)	Electronic	Minor editing privileges?	No
Who will republish the content?	Academic institution	Incidental promotional use?	No
Duration of Use	Life of current edition	Currency	USD
Lifetime Unit Quantity	Up to 499		
Rights Requested	Main product		

NEW WORK DETAILS

Title	Aldosterone Treatment Protects Connexin 30 And 43 Expression for Age-Related Hearing Loss	Institution name	University of South Florida
		Expected presentation date	2022-10-26
Instructor name	Jennifer Pineros		

ADDITIONAL DETAILS

Order reference number	N/A	The requesting person / organization to appear on the license	Jennifer Pineros

REUSE CONTENT DETAILS

Title, description or numeric reference of the portion(s)	Figure 3.	Title of the article/chapter the portion is from	Gap-junction channels dysfunction in deafness and hearing loss.
Editor of portion(s)	Martínez, Agustín D; Acuña, Rodrigo; Figueroa, Vania; Maripillan, Jaime; Nicholson, Bruce	Author of portion(s)	Martínez, Agustín D; Acuña, Rodrigo; Figueroa, Vania; Maripillan, Jaime; Nicholson, Bruce
Volume of serial or monograph	11	Issue, if republishing an article from a serial	2
Page or page range of portion	309-322	Publication date of portion	2009-02-01